Organic & Biomolecular Chemistry

ROYAL SOCIETY OF CHEMISTRY

REVIEW

View Article Online
View Journal

Cite this: DOI: 10.1039/d6ob00420b

Photoactive chiral structures for light-driven enantioselective carbon–carbon bond-forming reactions

Vijay Kumar S, A. Hameed Ibrahim and Anjan Das *

Asymmetric photocatalysis has emerged as a powerful strategy for forming enantioselective carbon–carbon bonds under mild conditions with high levels of enantioselectivity. Within this area, photoactive chiral systems represent an attractive and useful approach, as they eliminate the need for additional photosensitizers by combining the ability of light absorption and chiral induction within a single catalyst framework. Such catalysts act as chiral photosensitizers, enabling efficient harvesting of suitable light, generation of reactive excited states, and stereoselective bond formation. Recent studies demonstrate the effectiveness of this strategy in enantioselective C–C bond-forming reactions such as radical additions, cycloadditions, and cross-couplings. These methods improve efficiency and atom economy while broadening the scope of complex molecule synthesis. This review summarizes recent advances, mechanistic insights, and prospects of photocatalytic enantioselective C–C bond formation using self-sensitizing chiral systems, with relevance to drug discovery and fine chemical synthesis.

Received 13th March 2026,
Accepted 14th April 2026

DOI: 10.1039/d6ob00420b

rsc.li/obc

1. Introduction

Carbon–carbon (C–C) bond formation is one of the most fundamental and essential transformations in organic synthesis, serving as the cornerstone for constructing complex molecular architectures, including pharmaceuticals, agrochemicals, and materials.[1] Traditional methods for asymmetric C–C bond formation rely on organocatalysis, transition metal catalysis, or enzymatic catalysis for the synthesis of enantiopure products.[2]

Photocatalysis utilizes suitable light to generate highly reactive intermediates under mild conditions, enabling new reaction pathways that are otherwise challenging to achieve.[3] The combination of photocatalysis with asymmetric catalysis, often referred to as asymmetric photocatalysis, has opened new pathways for achieving stereoselective transformations with excellent enantiocontrol as well as diastereocontrol.[4] This

Department of Chemistry, SRM Institute of Science & Technology, Kattankulathur, Tamil Nadu 603203, India. E-mail: anjand@srmist.edu.in; Tel: +91 44 27417777

Vijay Kumar S

Mr Vijay Kumar S obtained his B.Sc. in Chemistry from A.M. Jain College (under the University of Madras) in 2022. He received his M.Sc. in General Chemistry from Vels Institute of Science, Technology and Advanced Studies in 2024. Then, he joined SRM Institute of Science and Technology in 2025 for his Ph.D. studies under the supervision of Dr Anjan Das. His current research interests include the photocatalytic synthesis of new enantioenriched heterocycles and various photocatalytic coupling reactions for drug discovery.

A. Hameed Ibrahim

Mr A. Hameed Ibrahim obtained his B.Sc. in Chemistry from Jamal Mohamed College (Autonomous) (under Bharathidasan University) in 2022. He received his M.Sc. in Chemistry from B.S. Abdur Rahman Crescent Institute of Science and Technology (Deemed University) in 2024. Then, he joined SRM Institute of Science and Technology in 2025 for his Ph.D. studies under the supervision of Dr Anjan Das. His current research interests include the photocatalytic synthesis of new enantioenriched heterocycles and various photocatalytic coupling reactions for drug discovery.

approach takes advantage of excited-state intermediates, single-electron transfer (SET) processes, energy transfer, or radical-pairing mechanisms to enable bond formation with high selectivity.

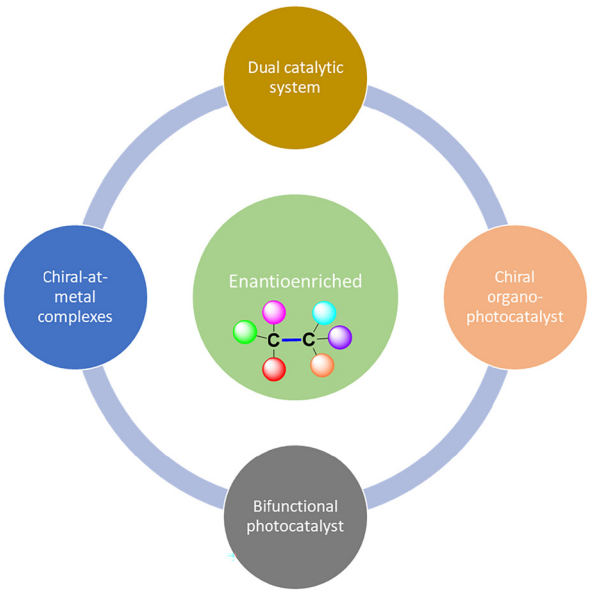

Fig. 1 Approaches to achieve the enantioenriched carbon–carbon bond formation.

Anjan Das

Dr Anjan Das obtained his B.Sc. in Chemistry (Honors) from Krishnath College (under Kalyani University) in 2007. He received his M.Sc. in Organic Chemistry from the University of Kalyani in 2009. Then, he pursued his Ph.D. in asymmetric catalysis at CSIR-CSMCRI in 2009. He conducted his postdoctoral research (2014–2017) at Florida State University with Prof. Kenneth Hanson, focusing on asymmetric excited-state proton transfer. Then, he worked with Prof. Iain Coldham at the University of Sheffield as a Newton International Postdoctoral Fellow on photocatalysis and kinetic resolution to obtain enantiopure heterocycles. He was appointed as Assistant Professor (Research) in the Department of Chemistry, SRM Institute of Science and Technology in 2023. His current research interests include the photocatalytic synthesis of new enantioenriched heterocycles, carbon dioxide utilization and the development of new methodologies.

As depicted in Fig. 1, key strategies developed for photocatalytic asymmetric C–C bond formation reactions can be mainly categorized into four routes. In the chiral organophotocatalytic strategy, the photosensitization and chiral induction originate from a single photoactive chiral molecule, which includes chiral amines, phosphoric acids, and thioureas, preferably following the primary asymmetric photocatalytic routes (Fig. 2).[5] Generally, substrates bind to the catalyst through hydrogen bonding or ionic interactions. In dual catalysis, photocatalysts (achiral transition metal complexes or organic dyes) and chiral organic molecules are separate entities that work synergistically to achieve asymmetric C–C bond formation *via* a secondary asymmetric photocatalytic route.[6] This strategy successfully allows many enantioselective cross-coupling reactions, where light-driven SET initiates radical recombination and energy transfer (EnT) enables asymmetric cycloaddition and rearrangement reactions that are difficult to control under conventional conditions. In the field of discrete chiral photocatalysts for asymmetric organic reactions, photoactive chiral organic molecules and several metal complexes featuring both chiral and non-chiral ligands have been shown to achieve excellent stereocontrol following the primary asymmetric photocatalytic route.[7] This success is likely due to the direct interaction between the substrates or reagents and the central transition metal. Two common strategies are documented to generate chiral metal complexes as discrete photocatalysts. The first strategy involves using a chiral organic ligand coordinated with an appropriate metal. The second, known as "chiral-at-metal", involves coordinating achiral organic ligands with a metal to form an octahedral complex (Werner complexes), where the overall structure of the complex itself exhibits chirality. In the case of electron donor–acceptor (EDA) complexes, the formation of the EDA takes place in the ground state between the chiral ligand and the substrates for the formation of an active photocatalyst.[8] Finally, bifunctional chiral photocatalysts are specialized catalysts that integrate two distinct functional components: a photocatalytic unit, which absorbs light and initiates photochemical transformations, typically through single-electron transfer (SET) or energy transfer (EnT) mechanisms *via* a secondary asymmetric photocatalytic route (Fig. 2), and a chiral-inducing unit, which provides a well-defined chiral environment to control the enantioselectivity of the reaction.[9]

While these published reviews provide important and comprehensive insights into enantioselective photocatalysis, they predominantly focus on broad catalytic concepts, catalyst development, or general mechanistic paradigms for dual catalytic systems. The purpose of this review article is to summarize advancements in homogeneous discrete chiral photocatalytic asymmetric C–C bond formation and its role in organic synthesis, specifically focusing on asymmetric C–C bond formation under visible-light irradiation, enabling a more targeted and practically useful understanding for synthetic chemists. We introduce a systematic classification based on various approaches to C–C bond construction, which allows direct comparison of diverse transformations across different

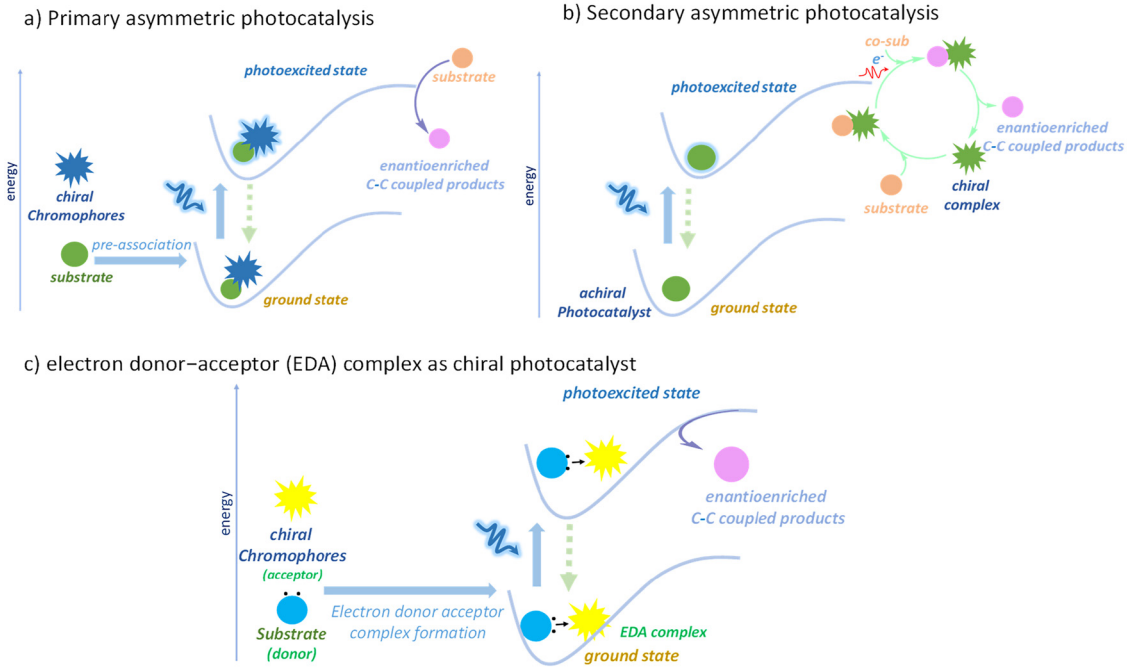

Fig. 2 General mechanism of asymmetric photocatalysis.

catalytic systems. Moreover, this review compiles recent developments in this class of chiral photocatalysts and mechanistic insights, helping researchers gain a deeper understanding, strengthen fundamental knowledge and stay updated. Other photocatalytic strategies for photocatalytic enantioselective carbon–carbon bond formation reactions are not included here as they have already been reported.[10] Additionally, this review addresses key challenges like low efficiency, limited substrate scope, and scalability for practical applications.

2. Chiral organo-photocatalysts

Chiral organo-photocatalysis has emerged as a powerful strategy for asymmetric carbon–carbon (C–C) bond formation, combining the advantages of organocatalysis and photocatalysis to achieve high enantioselectivity under mild conditions. Unlike traditional photocatalysis, which often relies on metal-based catalysts, organo-photocatalysis employs photoactive organic molecules, making it a sustainable and metal-free approach.[11] Chiral organic chromophores have previously been reported for photosensitized asymmetric isomerization of cyclic alkenes, followed by thermal cycloaddition with a suitable dienophile to facilitate asymmetric carbon–carbon bond formation.[12]

The photoactive chiral organic structure for enantioselective C–C bond formation was first reported by Schuster and coworkers. They developed a photocatalytic asymmetric [4 + 2] photocycloaddition of diene **1** and dienophile **2** using an axially chiral cyanoarene sensitizer **4** as an organo-photocatalyst. Their study revealed that, in polar solvents, the catalyst promotes radical cation Diels–Alder reactions, forming racemic products, while in nonpolar solvents, an enantioselective cycloadduct **3** (15% ee) is obtained (Scheme 1).[13] Mechanistic investigations suggest that electron transfer in polar solvents generates a radical-ion pair, whereas in nonpolar solvents, an exciplex is formed. Time-resolved fluorescence studies indicated the presence of two diastereomeric catalyst–styrene exciplexes, with enantioselectivity attributed to differences in their excited-state lifetimes.

Bach and coworkers made a significant advancement in enantioselective photocatalytic C–C bond-forming reactions by integrating a suitable sensitizer into a chiral template. They accomplished this by incorporating an aromatic ketone sensitizer into the chiral Kemp's acid motif while maintaining its essential hydrogen-bonding functionality, enabling it to act as a discrete chiral organo-photocatalyst. Using this approach, they have reported various enantioselective carbon–carbon bond-forming reactions by either electron transfer or energy transfer from the attached organic photosensitizer **22** (Scheme 2). This photocatalytic process proceeds *via* the primary asymmetric photocatalytic cycle (Fig. 2a), with pre-association between the catalyst and substrate occurring in the ground state prior to photoexcitation. Using chiral template **22a**, it was found to be optimal for an intramolecular enantioselective [2 + 2] photocycloaddition of 2-quinolone **5** *via* an energy transfer process (Scheme 2a).[14] The rigid cyclohexyl backbone and sterically demanding benzoxazole moiety restricted conformational flexibility, effectively facilitating facial differentiation in the prochiral substrate **5** and producing enantioselective product **6** with excellent selectivity (88% yield with 88% ee). Since hydrogen-bonding interactions are stronger at low temperatures, the highest enantioselectivity

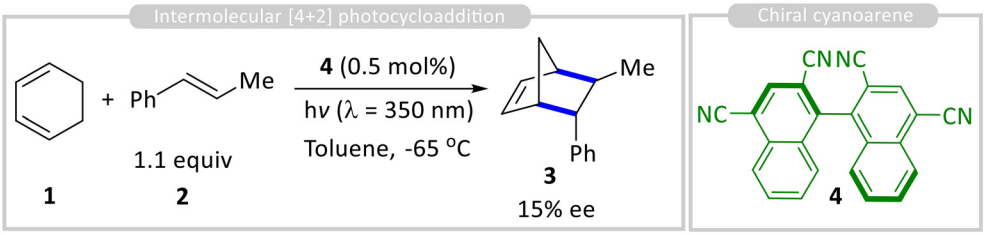

Scheme 1 Photoactive chiral cyanoarene for enantioselective [4 + 2] cycloaddition.

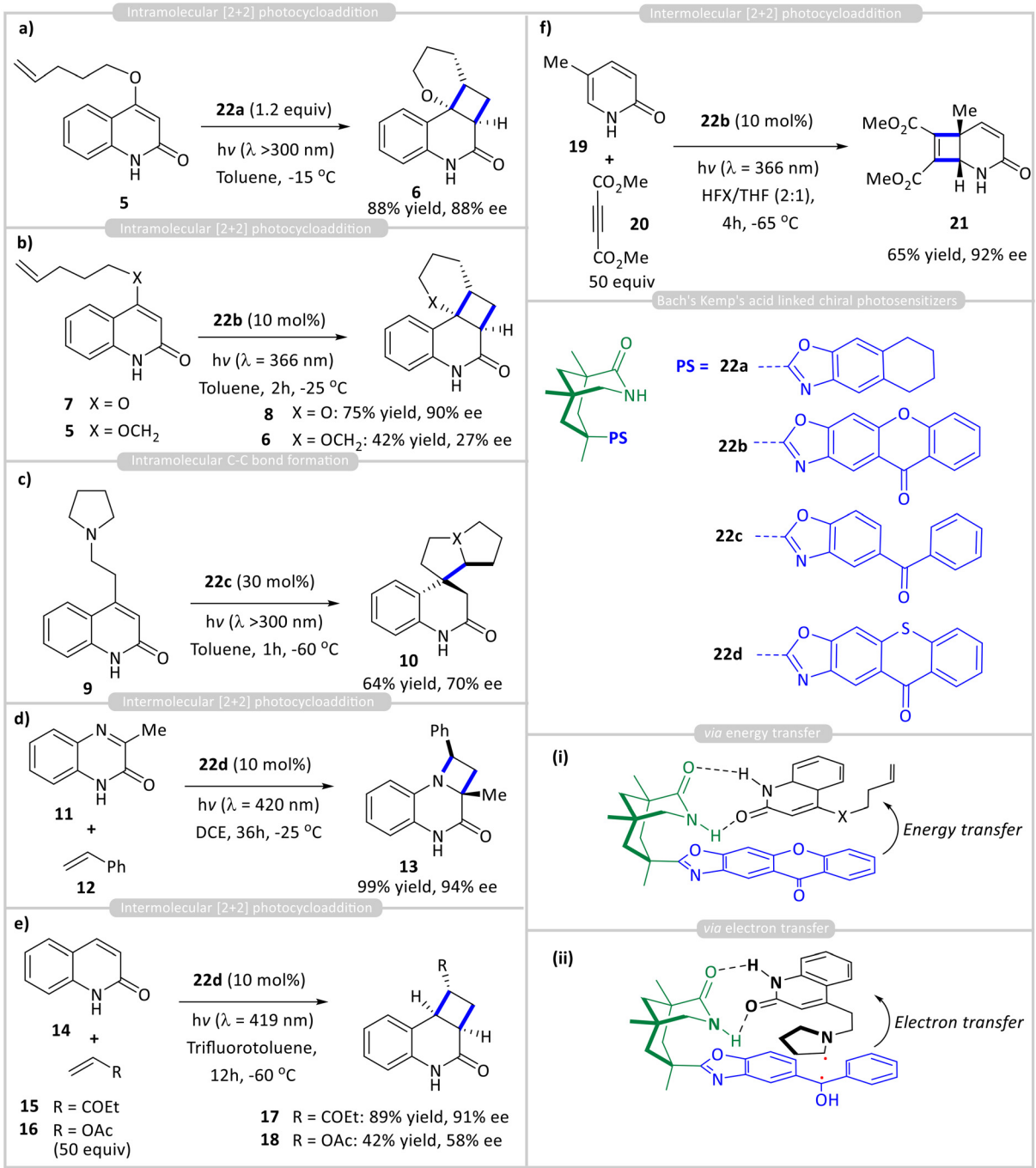

Scheme 2 Chiral organo-photocatalysis for enantioselective (a) & (b) intramolecular cycloadditions; (c) intramolecular C–C bond formation; and (d)–(f) intermolecular cycloaddition reactions.

was achieved under these conditions. Using the same strategy, they incorporated xanthone to develop organo-photocatalyst **22b**, which was then applied to the intramolecular [2 + 2] cycloaddition of quinolones **7** & **8**, forming cycloadducts **6** & **8**. They have achieved excellent yield (70%) and ee (90%), with substrate **7** significantly higher than substrate **8** (Scheme 2b).[15] As in both cases (**7** and **5**), catalyst **22b** remained fully bound to the substrate at the beginning of the reaction, indicating that ground-state association was not responsible for the change in selectivity. Instead, the enhanced selectivity was attributed to the efficiency of photosensitization and the rate of the subsequent reaction. Although the substrates absorb light at the irradiation wavelength, the xanthone photocatalyst **22a** has a much higher extinction coefficient than the substrates, enabling it to capture nearly all incident photons under the reaction conditions. Consequently, the racemic background reaction is significantly suppressed, resulting in high enantioselectivity.

In a previous study, using the electron transfer strategy, Bach *et al.* reported the intramolecular cyclization of pyrrolidine **9** to spirocycle **10** using 30 mol% of ketone catalyst **22c**, achieving 70% enantiomeric excess (ee) through a hydrogen-bonding mechanism and photoinduced electron transfer (PET) (Scheme 2c).[16] It is important to note that intermolecular photoreactions are significantly more challenging than their intramolecular counterparts due to the inherent competition between substrate dissociation and cyclization. Despite this difficulty, Bach successfully developed an intermolecular [2 + 2] photocycloaddition between cyclic imine **11** and styrene **12**, photocatalyzed by **22d** to produce the enantioselective cycloadduct **13** with 99% yield and 94% ee (Scheme 2d).[17]

Further studies on the intermolecular [2 + 2] photocycloaddition between quinolone **14** and various alkene coupling partners (**15** and **16**) revealed that the reaction, catalysed by **22d**, required 50 equivalents of the alkene to ensure that cyclization occurred before dissociation from the catalyst (Scheme 2e).[18] Based on this, it could be concluded that alkenes that react more slowly are expected to yield products with lower enantioselectivities. For example, vinyl acetate **16** reacts over an order of magnitude slower than ethyl vinyl ketone **15** when photosensitized by an achiral thioxanthone, resulting in significantly lower enantiomeric excess in the corresponding cycloadducts (91% ee *vs.* 58% ee).

In another study, they developed an intermolecular [2 + 2] photocycloaddition between pyridone **19** and acetylenedicarboxylates **20** that is catalyzed by **22b**. Since pyridone **19** does not absorb the irradiated light under these reaction conditions, the enantioselectivity does not strongly correlate with catalyst loading. However, a clear relationship was observed between the alkyne concentration and enantioselectivity. It was proposed that a higher concentration of the coupling partner facilitates a faster bimolecular reaction, reducing the likelihood of substrate dissociation and leading to improved enantioselectivity (Scheme 2f).[19]

Xanthone and thioxanthone catalysts were initially limited to lactam-containing substrates, delivering good efficiency and enantioselectivity. To broaden the range of compatible binding motifs, Bach and co-workers developed new catalysts that integrate a thioxanthone sensitizer into alternative chiral hydrogen-bonding scaffolds, such as BINOL-derived phosphoric acids **29a** and chiral thioureas **29b** (Scheme 3). Using BINOL-derived phosphoric acid **29a** as a chiral photocatalyst, an intermolecular [2 + 2] cycloaddition between carboxylic acid **23** and cyclopentene **24** was achieved with 61% yield and 86% ee (Scheme 3a).[20] In contrast, the thiourea-linked thioxanthone **29b** showed poor enantioselectivity (12% ee) in a sensitized 6π-electrocyclization. NMR studies confirmed that carboxylic acid **25** binds to catalyst **29a** under reaction conditions, while computational analysis suggests that the low enantioselectivity arises from multiple, energetically similar binding modes of the 1 : 1 complex. Additionally, thioxanthone catalyst **29a** effectively promoted the enantioselective photocycloaddition of *N*,*O*-acetal **26** and alkene **27**, affording 95% ee (Scheme 3b).[21] NMR analysis indicated that **26** exists in equilibrium between a cyclic *N*,*O*-acetal and a ring-opened imine form. Emission studies showed that the triplet energy of the iminium ion (51 kcal mol^{-1}) is lower than that of the thioxanthone catalyst (56 kcal mol^{-1}), supporting an exothermic energy transfer process.

Melchiorre and co-workers introduced an innovative approach to asymmetric photocatalysis based on electron donor–acceptor (EDA) complexes. In this method, an electron-rich donor and an electron-deficient acceptor interact in the ground state to form an EDA complex. This interaction results in the emergence of a new charge-transfer absorption band, which can be interpreted as an intra-complex electron transfer from the donor's HOMO to the acceptor's LUMO. Using this strategy, they reported enantioselective α-alkylation of aldehyde **30** with alkyl halide **31** to provide enantioselective **32** in 87% yield with 92% ee (Scheme 4a).[22] A chiral secondary amine forms an enamine intermediate, which interacts with an alkyl bromide to create a visible-light-absorbing EDA complex. Excitation triggers electron transfer, generating radicals. The chiral catalyst facilitates both photochemical initiation and enantioselective radical addition (Scheme 4e). Melchiorre and co-workers showed that bromomalonate **34** enables the α-alkylation of aldehydes **30** using amine organocatalyst **36**, achieving up to 94% ee and complete γ-selectivity for enals (Scheme 4b).[23] While an EDA complex was initially suspected, UV–vis studies ruled it out, and Stern–Volmer quenching confirmed a SET mechanism. The excited enamine reduces bromomalonate **34**, forming a malonyl radical that reacts with the ground-state enamine. Unlike EDA reactions, chain propagation occurs *via* bromine abstraction. The photochemical step serves only to initiate the radical chain (Scheme 4e). Alemán and co-workers reported a similar photo-organocatalytic reaction using a thioxanthone-substituted organocatalyst **39**, which efficiently produces alkylated aldehyde **37** with high yield (up to 99%) and enantioselectivity (up to 99%) (Scheme 4c).[24] In this reaction, rather than the enamine acting as the reducing agent, the thioxanthone catalyst **39** facilitates the reduction of bromomalonate **34**, initiat-

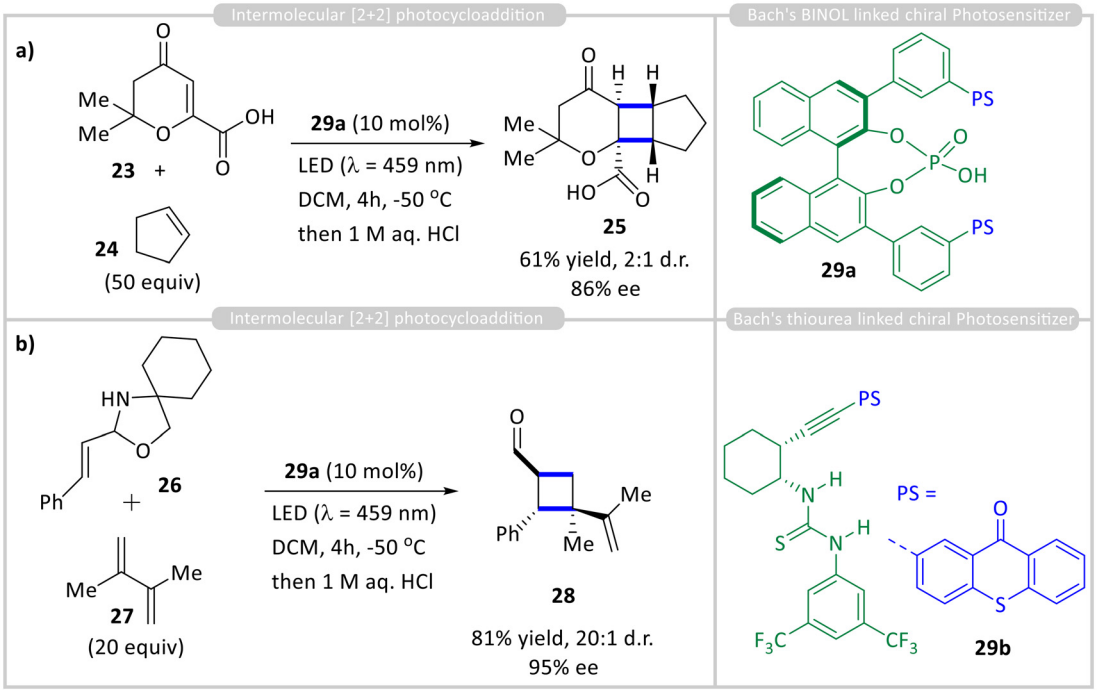

Scheme 3 Chiral BINOL-derived phosphoric acid and thiourea-linked thioxanthone-sensitised enantioselective (a) & (b) intermolecular [2 + 2] cycloaddition reactions.

ing the radical chain process. This mechanistic shift highlights the role of thioxanthone as a key photoredox mediator, broadening the scope of organocatalytic radical reactions and offering an alternative pathway for enantioselective α-alkylation of aldehydes. Other electron acceptors, like (phenylsulfonyl)-alkyl iodides, also worked well, yielding highly enantioselective products. A related photo-organocatalytic strategy was effectively extended to ketone substrate **40** using a cinchona-based primary amine catalyst **42** (Scheme 4d).[25] Electron-deficient benzyl bromide **31** functioned as a suitable electron acceptor, though the reaction remained limited to cyclic ketones as chiral enamine electron-donor precursors.

In 2017, Melchiorre and co-workers developed an asymmetric β-alkylation of enals using chiral iminium ions formed *in situ* from α,β-unsaturated aldehyde **43** and chiral amine catalysts **46** (Scheme 5a).[26] Unlike enamine photocatalysis, which involves nucleophilic intermediates, iminium photocatalysis leverages electrophilic iminium ions that become strong oxidants upon excitation. The proposed mechanism involves visible-light absorption by the iminium ion, which oxidizes an alkyl trimethylsilane **44**, generating radicals that undergo direct radical–radical coupling to form β-alkylated aldehyde **45** in up to 82% yield with 80% ee. This method provides selective 1,4-addition, improving upon traditional thermal iminium catalysis, which often yields a mixture of 1,2- and 1,4-addition products. Toluene **48** can reductively quench the excited-state iminium ion, enabling the formation of β-benzylated aldehyde **49** from enals generated from **47** and **50** (Scheme 5b).[27] Upon oxidation, toluene's benzylic C–H bond becomes highly acidic, with an estimated pK_a of −13 in CH_3CN.[28] Deprotonation generates a benzyl radical, which then undergoes radical–radical coupling with the β-enaminyl radical intermediate. $Zn(OTf)_2$ was essential for this reaction, with Zn^{2+} facilitating iminium formation and the triflate counterion assisting in the deprotonation of the photogenerated toluene radical cation.

Scalability remains a key limitation of chiral organo-photocatalysts due to common photochemical challenges such as poor light penetration, non-uniform irradiation in batch systems, high catalyst loadings, and limited photostability under prolonged exposure. Continuous-flow photochemistry offers a promising solution by improving light distribution, heat dissipation, and reproducibility, making it more suitable for large-scale synthesis.

However, translating these reactions from batch to flow is still underexplored. Issues like catalyst solubility, adsorption or deactivation in flow channels, and the need to optimize residence time and light intensity must be addressed. Advancing robust, flow-compatible chiral organo-photocatalysts, alongside systematic reaction engineering, will be crucial for achieving scalable asymmetric synthesis.

3. Chiral metal complexes

Chiral metal complexes have emerged as powerful discrete photocatalysts for various enantioselective organic transformations, combining photocatalysis and asymmetric induction within a single catalytic framework.[29,7a] These complexes, typi-

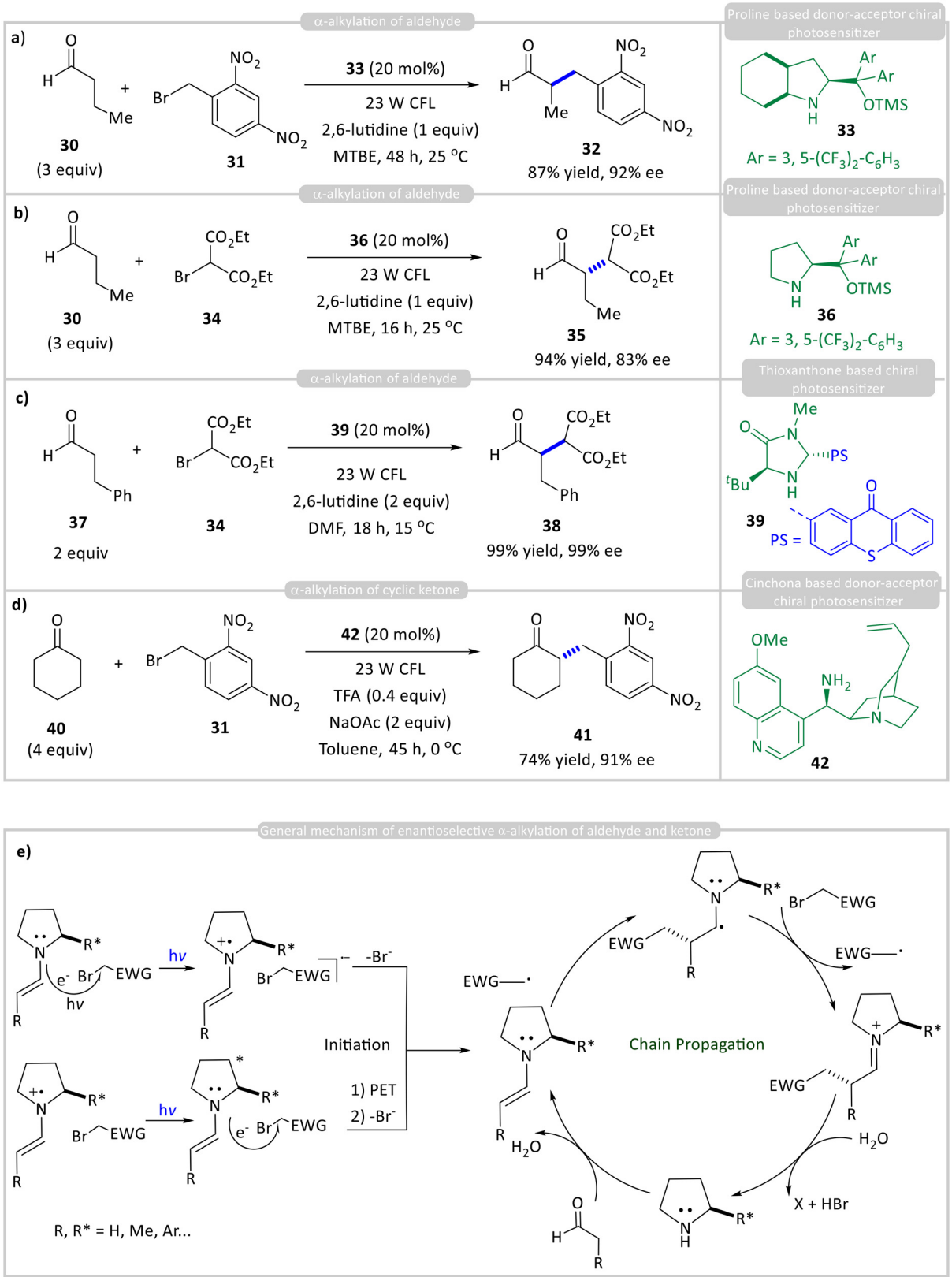

Scheme 4 Chiral organo-photocatalyzed enantioselective (a)–(c) α-alkylation of aldehydes; (d) α-alkylation of ketones; and (e) general reaction mechanism.

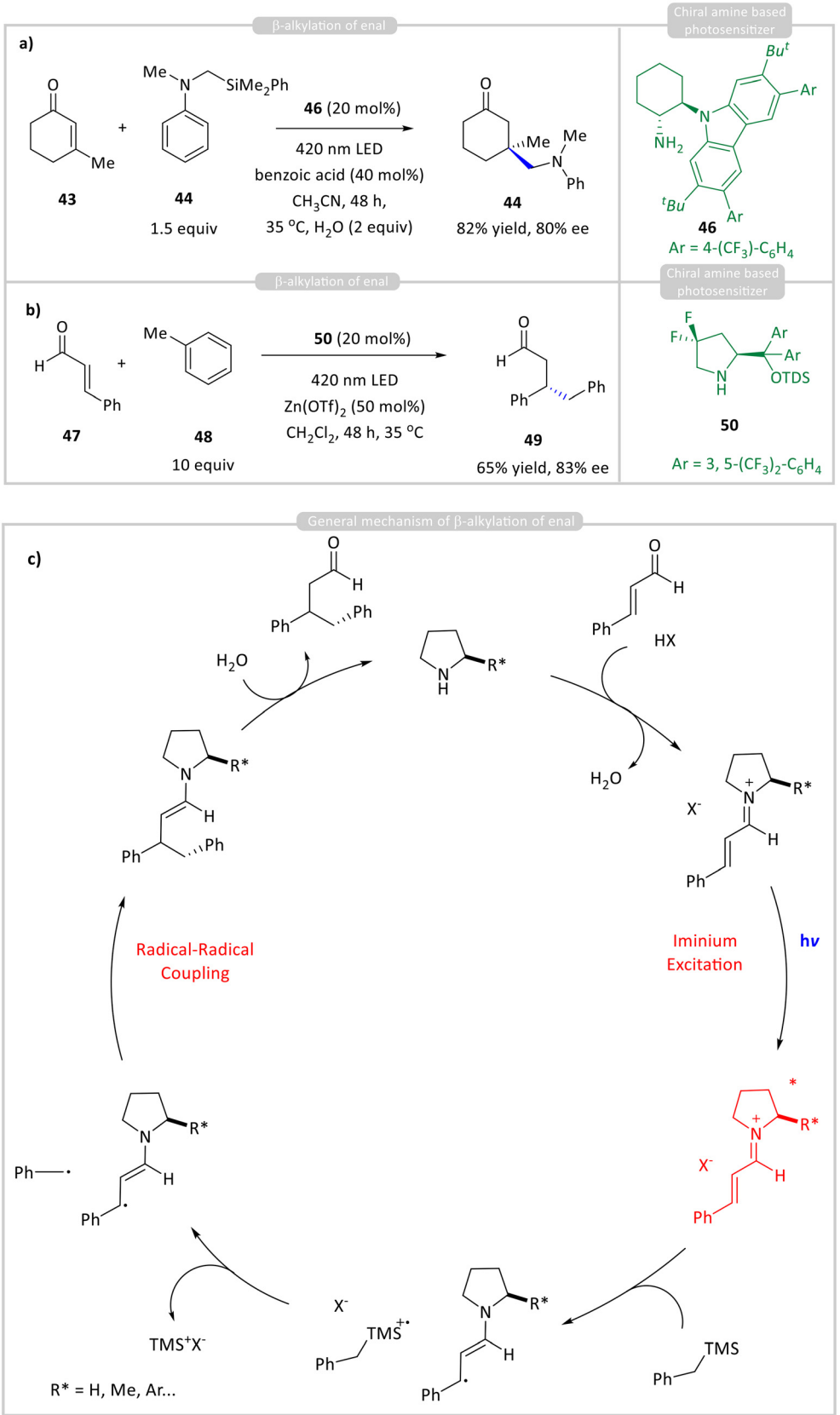

Scheme 5 Chiral organo-photocatalyzed enantioselective (a) & (b) β-alkylation of enals; and (c) general mechanism.

cally based on transition metals such as Ru, Ir, or Cu, incorporate enantiopure ligands that create a well-defined chiral environment while simultaneously facilitating photoinduced electron transfer (SET) or energy transfer (EnT) processes. Additionally, these complexes can be generated from transition metals and achiral ligands (chiral-at-metal) as active chiral photocatalysts.[30] Meggers pioneered the use of helically chiral iridium(III) polypyridyl complexes as enantioselective photocatalysts for a variety of synthetically important transformations. These catalysts can be easily prepared in stereochemically pure form using a chiral auxiliary approach and have been shown to be resistant to racemization.[31] The metal centre (*e.g.*, Ru or Rh) becomes a stereogenic centre due to the arrangement of achiral ligands in a chiral fashion. These complexes exist in Λ (lambda) or Δ (delta) configurations, and the metal's spatial arrangement imparts chirality (Fig. 3).[32] These Ir/Rh complexes serve two roles simultaneously: as photocatalysts, they absorb visible light and enter an excited state; and as chiral Lewis acids, they coordinate and orient the substrate in a defined chiral environment, enabling stereocontrol.

3.1 Rhodium/iridium incorporated chiral metal complexes

Meggers' group has reported a series of photocatalytic enantioselective carbon–carbon bond formation reactions using these Ru- and Rh-based chiral-at-metal complexes with a pre-association mechanism (Fig. 2a), where the substrate binds to the chiral catalyst before the photochemical event (light excitation) (Scheme 6). This binding or pre-association plays a central role in controlling enantioselectivity. This strategy avoids issues with diffusion-controlled processes, where radicals formed freely in solution can react randomly, reducing enantioselectivity. This interaction often involves coordination to the metal centre (as a Lewis acid) or hydrogen bonding with the ligand framework (Yoon's strategy). Upon photoexcitation, the chiral metal complex bound with substrate becomes redox-active and initiates the reaction, either by single-electron transfer (SET) or energy transfer. Because the substrate is already held in a chiral pocket, the reactive intermediate (radical, cation, *etc.*) formed after excitation undergoes diastereoselective steps as the substrate–catalyst complex is already entity; hence, the subsequent reactions are diastereoselective, such as radical recombination, bond formation, or nucleophilic attack. Meggers' pioneering studies revealed that Λ-**51b** efficiently catalyses the highly enantioselective α-alkylation of 2-acylimidazolyl ketone **53** with electron-deficient benzyl bromide **54** radical precursors, affording the α-alkylated product **55** with excellent enantioselectivity (99% ee) (Scheme 6a).[33] In follow-up studies, they utilized a modified analogue, Λ-**51c**, to achieve the enantioselective α-trichloromethylation of *N*-phenyl-2-acylimidazoles **56**, affording enantiopure α-trichloromethylated products **55** *via* the same mechanistic pathway (Scheme 6b).[34] Using the same strategy, they reported the desilylative oxidation of α-silyl amines **60** using the substrate **59**-bound chiral-at-metal Ir(III) complex **Δ-51a** as the active chiral photocatalyst (Scheme 6c).[35] Chiral-at-metal Rh(III) photocatalysts exhibit superior versatility over first-generation iridium complexes. Using Λ-**51a**, *N*,*N*-dialkylaniline **62** was oxidized to a radical cation, which rapidly deprotonated to form an α-amino radical. Subsequent air oxidation generated an iminium ion that reacted asymmetrically with enolates from **59**, affording product **63** in up to 80% yield and 95% ee (Scheme 6d).[36] A photogenerated alkyl radical from Hantzsch ester **66** for asymmetric addition to α,β-unsaturated ketone derivatives **64**, using the chiral-at-metal Rh(III) complex Λ-**52a** to obtain product **63**, was successfully demonstrated by Meggers' group (Scheme 6e).[37] Furthermore, Meggers and co-workers reported the stereoselective asymmetric coupling of racemic α-chloro-imidazol-2-yl ketones **67** with *N*-arylglycines **68** using the chiral photocatalyst **Δ-52b** (Scheme 6f).[38] Upon photoexcitation, the chiral-at-rhodium complex generates radicals from both substrates, which undergo enantioselective radical–radical coupling to afford β-amino ketone **69** with up to 93% ee. An asymmetric [3 + 2] cycloaddition was achieved using the chiral-at-Rh(III) photocatalyst **Δ-52b**, wherein cyclopropyl imidazolyl ketone **70** reacted with various alkenes and alkynes **71** to afford highly enantioselective cyclopentanes and cyclopentenes **72** (Scheme 6g).[39] Through a series of experiments, the authors have proposed a plausible mechanism for the catalytic reaction. X-ray crystallographic analysis confirms that the substitutionally labile acetonitrile ligands of **Λ/Δ-51/52** are replaced by the bidentate substrate while preserving the stereochemical integrity of the metal centre. In the presence of a base, deprotonation generates a chiral enolate complex. Furthermore, Stern–Volmer luminescence quenching studies, together with electrochemical measurements, suggest that this intermediate functions as the active photocatalyst, absorbing visible light to reduce the electron-deficient alkyl bromide. The resulting alkyl radical subsequently attacks the enolate within a chiral environment, affording the enantiopure product.

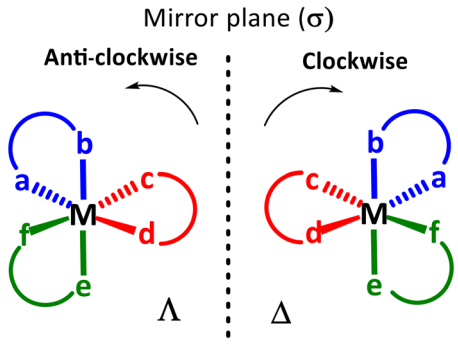

Fig. 3 Octahedral chiral-at-metal complexes.

3.2 Iridium-incorporated chiral metal complexes with H bonding

Inspired by Meggers' work, Yoon developed Ir-based chiral-at-metal complexes with hydrogen-bonding functionality through the ligand. They have followed the pre-association *via* hydrogen bonding. The Ir(III) complex contains ligands that can

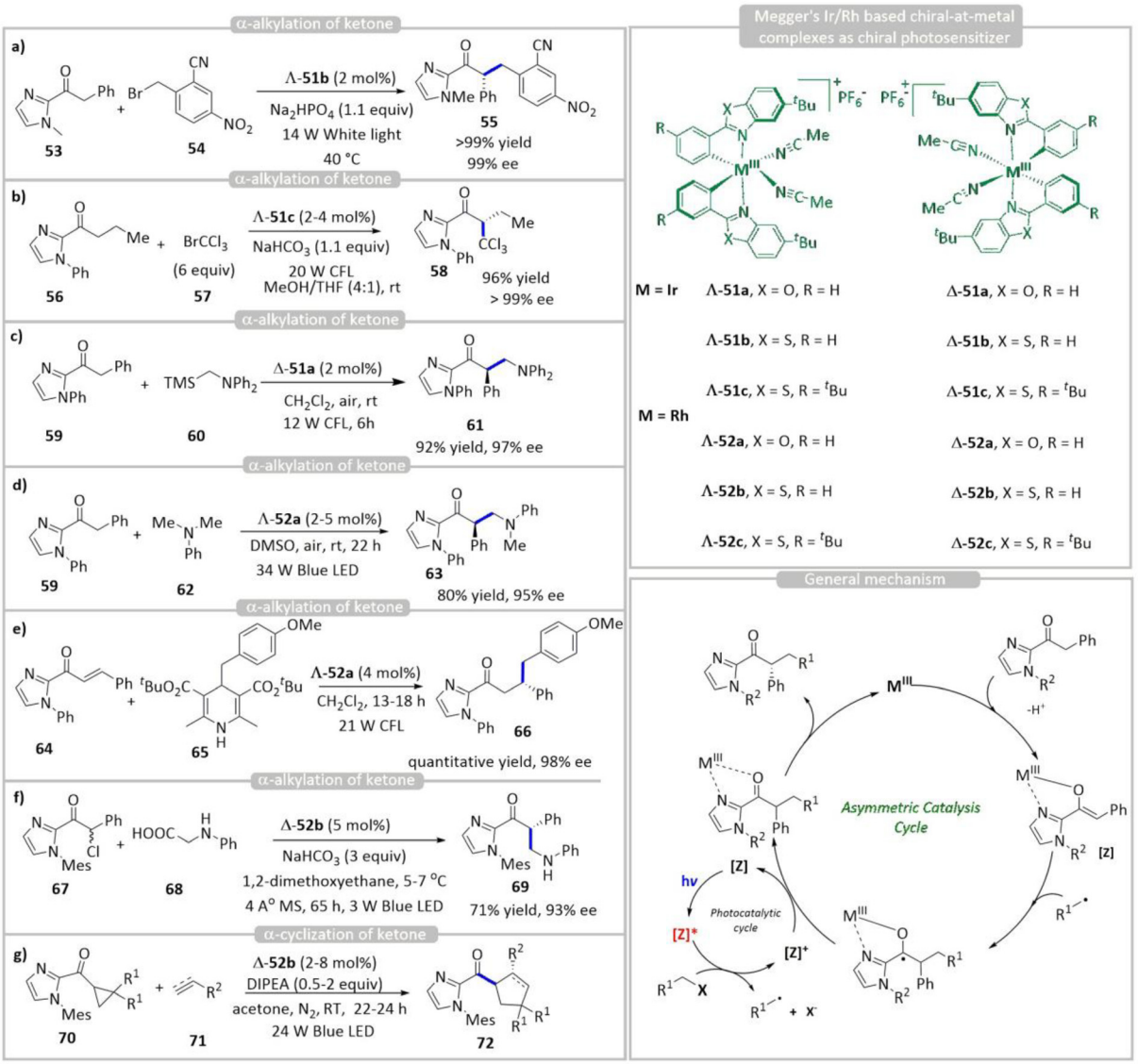

Scheme 6 Chiral-at-metal complexes as discrete photocatalysts for asymmetric (a–g) α-alkylation of ketones.

form hydrogen bonds with carbonyl or amide-containing substrates. This pre-association orients the substrate in a defined spatial arrangement within the chiral pocket of the catalyst. Upon irradiation with visible light (blue LED), the Ir(III) complex bound with the substrate is excited to its triplet MLCT (metal-to-ligand charge transfer) state. This excited state has a long lifetime and can transfer energy to the bound substrate. Unlike photoredox SET processes, Yoon's approach often uses energy transfer to excite the bound alkene substrate to its triplet state, initiating a [2 + 2] cycloaddition. The bound substrate undergoes triplet excitation while remaining hydrogen-bonded and geometrically restricted. The excited substrate reacts with another alkene or a conjugated system in a [2 + 2] fashion, forming a cyclobutane ring. Because the substrate is fixed in the chiral environment during excitation and reaction, the cycloaddition proceeds with high facial selectivity, affording enantioselective cyclobutanes (Scheme 7). Using the chiral iridium photosensitizer, Λ-**73a**, a photocatalytic intramolecular asymmetric [2 + 2] cycloaddition of quinolone substrate **74** generated enantioselective cycloadduct **75** with excellent yield (>99%) and enantioselectivity (90% ee) (Scheme 7a).[40] Computational studies, including DFT and transient absorption spectroscopy, have revealed that π–π stacking interactions between the Ir complex and the substrate further stabilize the complex and influence enantioselectivity. They further applied this strategy to the photocatalytic asymmetric intermolecular [2 + 2] cycloaddition between 3-isopropoxyquinolone **76** and maleimide **77**. Using a slightly modified chiral photocatalyst, Λ-**73b**, the reaction delivered cyclobutane **78** in high yield with enantioselectivity of up to 97% ee (Scheme 7b).[41] Mechanistic studies revealed a rebound pathway for this intermolecular [2 + 2] photocycloaddition.

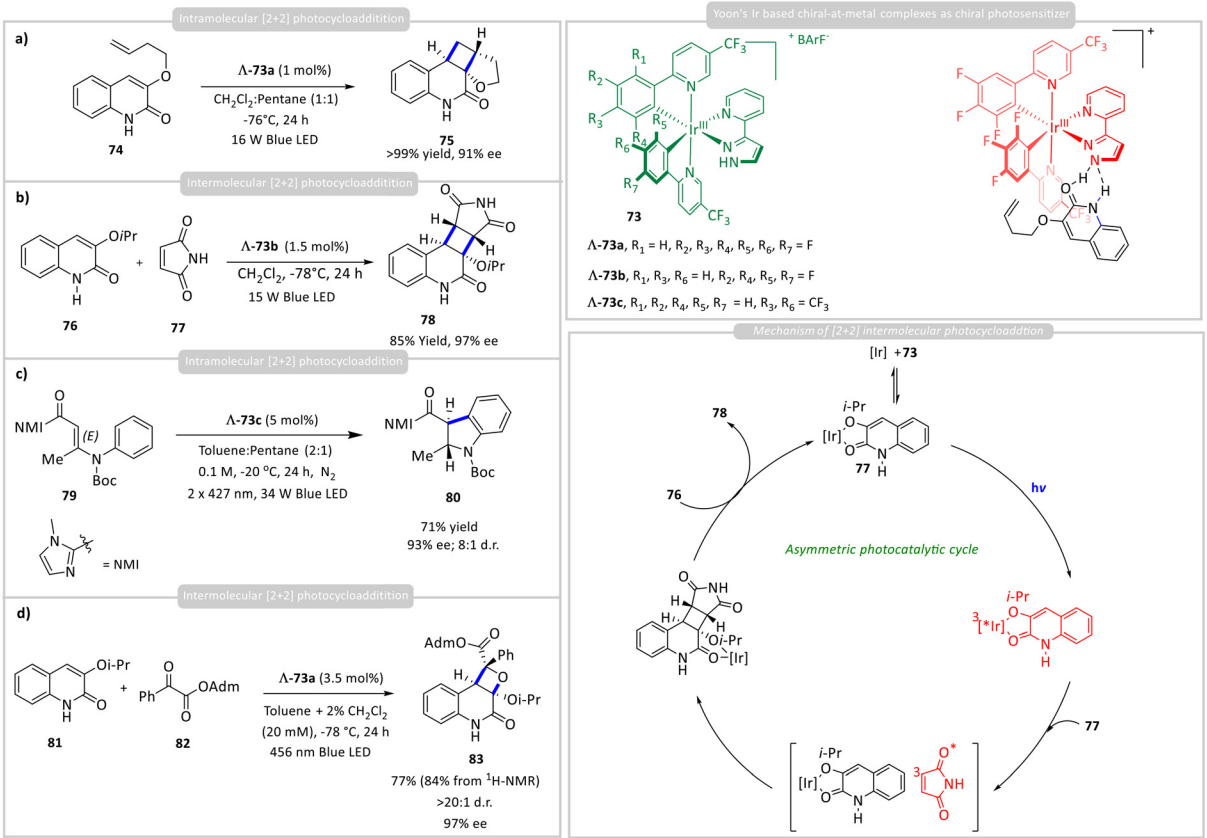

Scheme 7 Enantioselective (a) & (c) intra- and (b) & (d) intermolecular [2 + 2] photocycloadditions with a chiral hydrogen-bonding iridium photosensitizer.

While the chiral Ir complex preferentially coordinates to quinolone **76**, the energy transfer is directed to the maleimide **77** partner. The resulting triplet-excited maleimide **79** then engages the bound quinolone **78** in a stereoselective fashion, affording cyclobutane **78** with excellent enantioselectivity (up to 97% ee). They next reported an enantioselective **6π** photoelectrocyclization of substrates **79** bearing a *C*-acylimidazole unit, enabled by a single hydrogen-bonding chiral Ir(III) photosensitizer, Λ-**73c** (Scheme 7c).[42] Key to this transformation was the rational design of a strong hydrogen-bonding interaction between the pyrazole moiety of photocatalyst **Λ-73c** and the imidazolyl ketone group of the substrate. This interaction effectively controlled stereoselectivity, affording indoline products **80** in good yields with excellent enantiomeric excesses (>90% ee).

3.3 Ruthenium/iridium-incorporated chiral metal complexes attached with chiral auxiliaries

A few groups have developed Ir(III)/Ru(II)-based photosensitizers integrated with chiral hydrogen-bonding ligands for asymmetric photocatalysis. For instance, Bach and co-workers introduced an iridium catalyst **86** bearing a chiral lactam-functionalized bipyridine ligand, which showed limited stereocontrol in the reductive cyclization of α-bromo carbonyls **84**, yielding cyclized product **85** with low enantioselectivity (<10% ee) due to competing hydride bromination (Scheme 8a).[43] However, better results were achieved in the energy-transfer-mediated rearrangement of spiroepoxide **87**, producing ketone **88** with excellent yield and 29% ee (Scheme 8b). In a related strategy, Ceroni, Lombardo, and Cozzi developed a supramolecular photocatalyst **93** combining an Ir(III) sensitizer with a chiral imidazolidinone organocatalyst. This system enabled asymmetric alkylation of aldehydes **90** with bromo compound **36**, achieving up to 84% yield and 70% ee of product **91** (Scheme 8c).[44] Separate addition of the two components significantly reduced both the yield (57%) and enantioselectivity (59%), highlighting the importance of spatial proximity. The mechanism involves photoinduced reductive quenching of the Ir(III) complex, generating an alkyl radical that reacts with an enamine intermediate, though no definitive evidence supports a radical chain process. Ohkubo and co-workers introduced chiral substituents on bipyridine ligands to develop Ru(II) complex **95** with enhanced stereocontrol. They further demonstrated that **Δ-95** catalyses the atroposelective oxidative coupling of 2-naphthol **93** to form BINOL **94** with 33% yield and 16% ee (Scheme 8d).[45,46] The reaction proceeds *via* photoexcited **Δ-95**, which is oxidation by $Co(acac)_3$, generating Ru(III), which in turn oxidizes **93** to initiate the coupling.

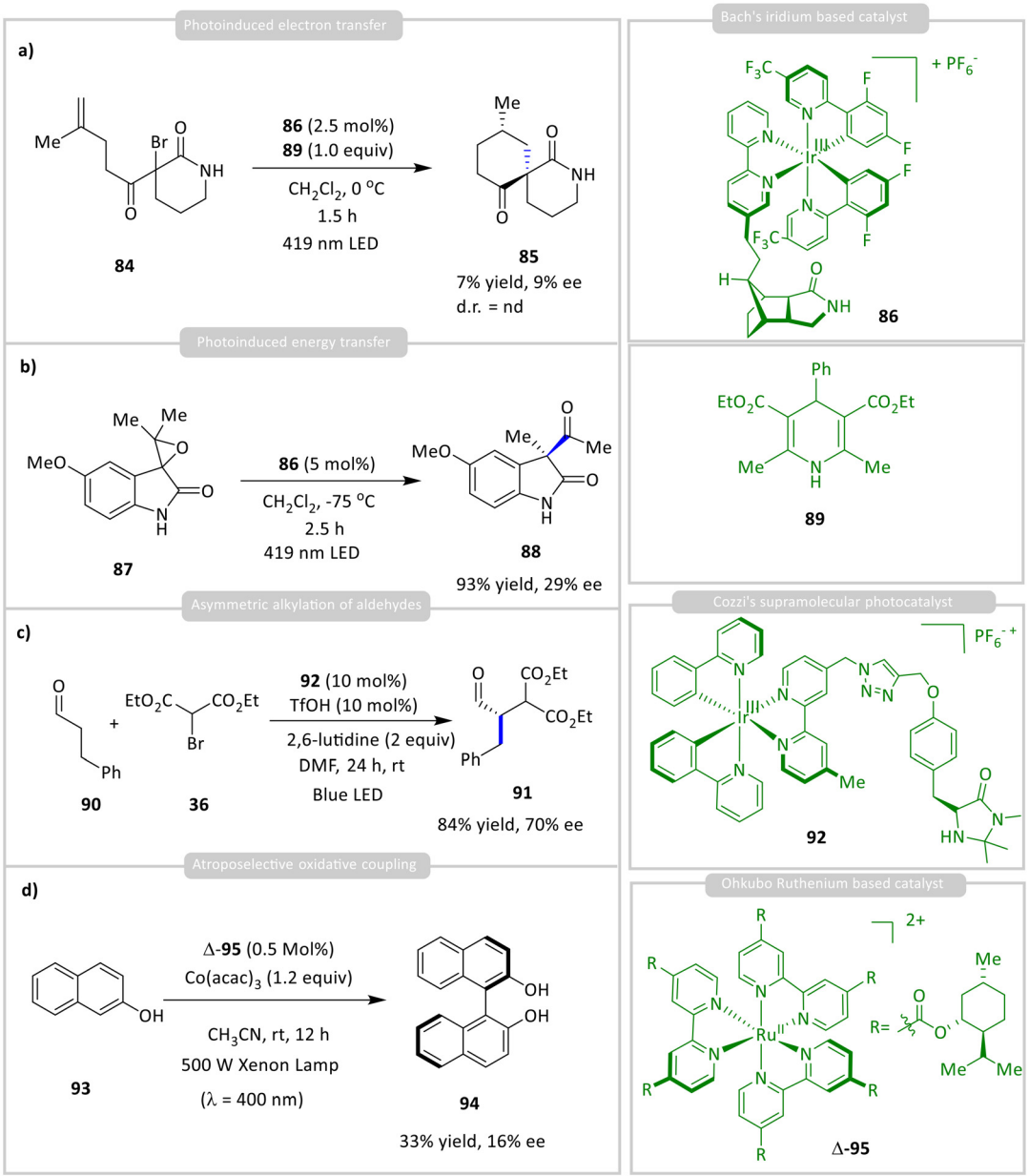

Scheme 8 Asymmetric (a) PET, (b) energy-transfer, (c) asymmetric alkylation and (d) atroposelective oxidative coupling reactions using a chiral hydrogen-bonding ligand.

3.4 Other iridium/rhodium-incorporated chiral metal complexes

A few groups have successfully applied chiral bifunctional photocatalysts that combine ionic interactions between a photosensitizer and a chiral catalyst for asymmetric C–C bond formation. Ooi and co-workers developed a system using a cationic Ir(III) photocatalyst **99** paired with a chiral hydrogen-bonding borate counteranion for an asymmetric [3 + 2] cycloaddition (Scheme 9a).[47] The strained *N*-cyclopropylurea substrate **96** binds to the chiral borate **99**, accelerating the reaction compared to the racemic Ir complex. Notably, the Ir centre's chirality had no impact on selectivity, as both Δ and Λ isomers gave similar results. The reaction proceeds *via* photoinduced oxidation of the borate-bound urea to form a radical-ion pair intermediate, which selectively reacts with α-substituted styrene **97** to yield cyclopentane products **98** with up to 98% yield and 93% ee. This strategy enables efficient access to α-quaternary β-amino acids, which are key intermediates for β-peptides and peptidomimetics.

Separately, Melchiorre and co-workers reported enantioselective allylic substitutions using iridium complex **103**, which acts both as a privileged organometallic intermediate and as a photoredox catalyst (Scheme 9b).[48] Upon excitation, it

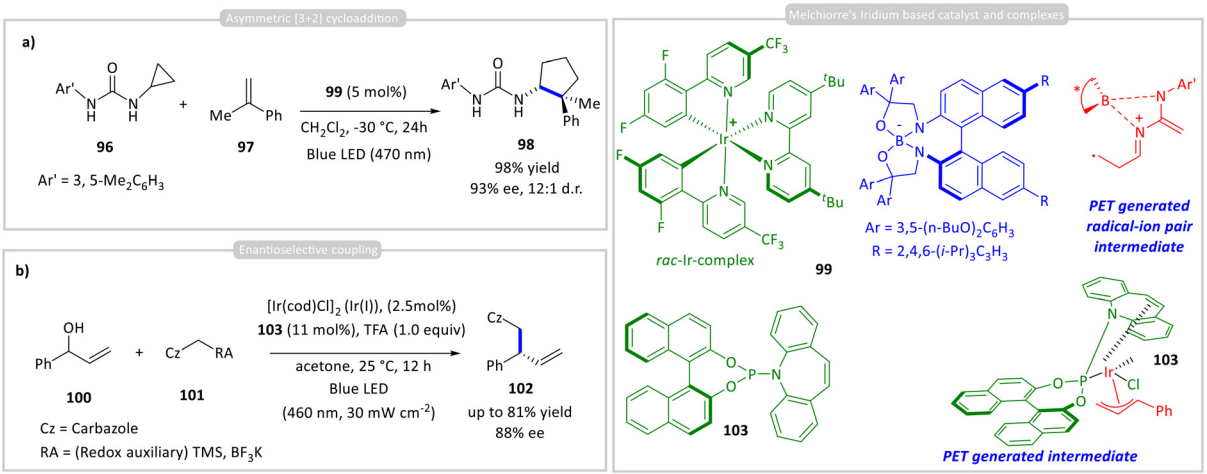

Scheme 9 (a) Asymmetric [3 + 2] cycloaddition; (b) enantioselective coupling using iridium-chiral borate ion pairs as a chiral photocatalyst and an (η^3-alyl)iridium(III) photocatalyst.

oxidizes carbazoles **101** bearing cleavable redox auxiliaries, generating stabilized radicals that undergo enantioselective coupling with an (η^3-allyl)Ir(II) complex *via* reductive elimination, affording product **102** in high yield and enantioselectivity.

Kang and co-workers developed an asymmetric conjugate radical addition of photogenerated α-amino radicals from tetrahydroisoquinoline **105** to α,β-unsaturated 2-acylimidazoles **104** coordinated to a chiral rhodium catalyst (**Λ-107**), achieving excellent yields (up to 92%) and enantioselectivity (>99% ee)

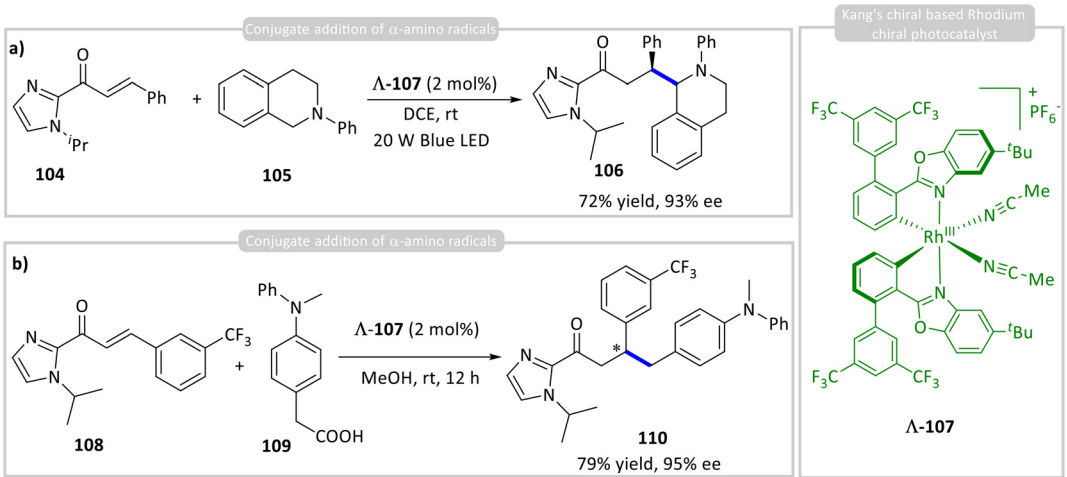

Scheme 10 Asymmetric photocatalytic (a) & (b) conjugate addition of α-amino radicals with Michael acceptors using a photoactive rhodium-amine catalyst.

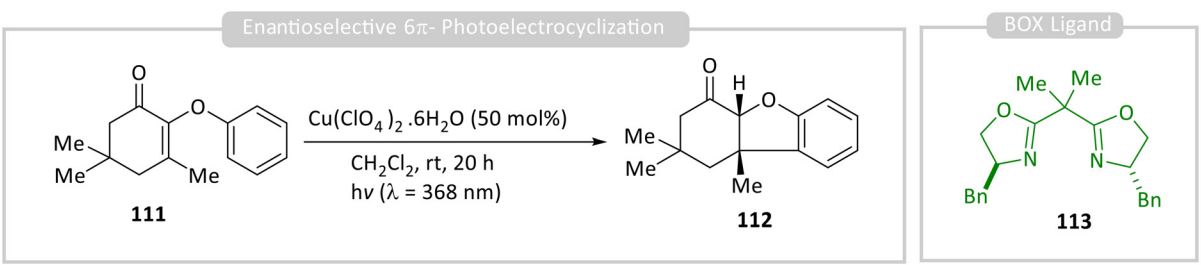

Scheme 11 Enantioselective 6π-photoelectrocyclization using a BOX ligand.

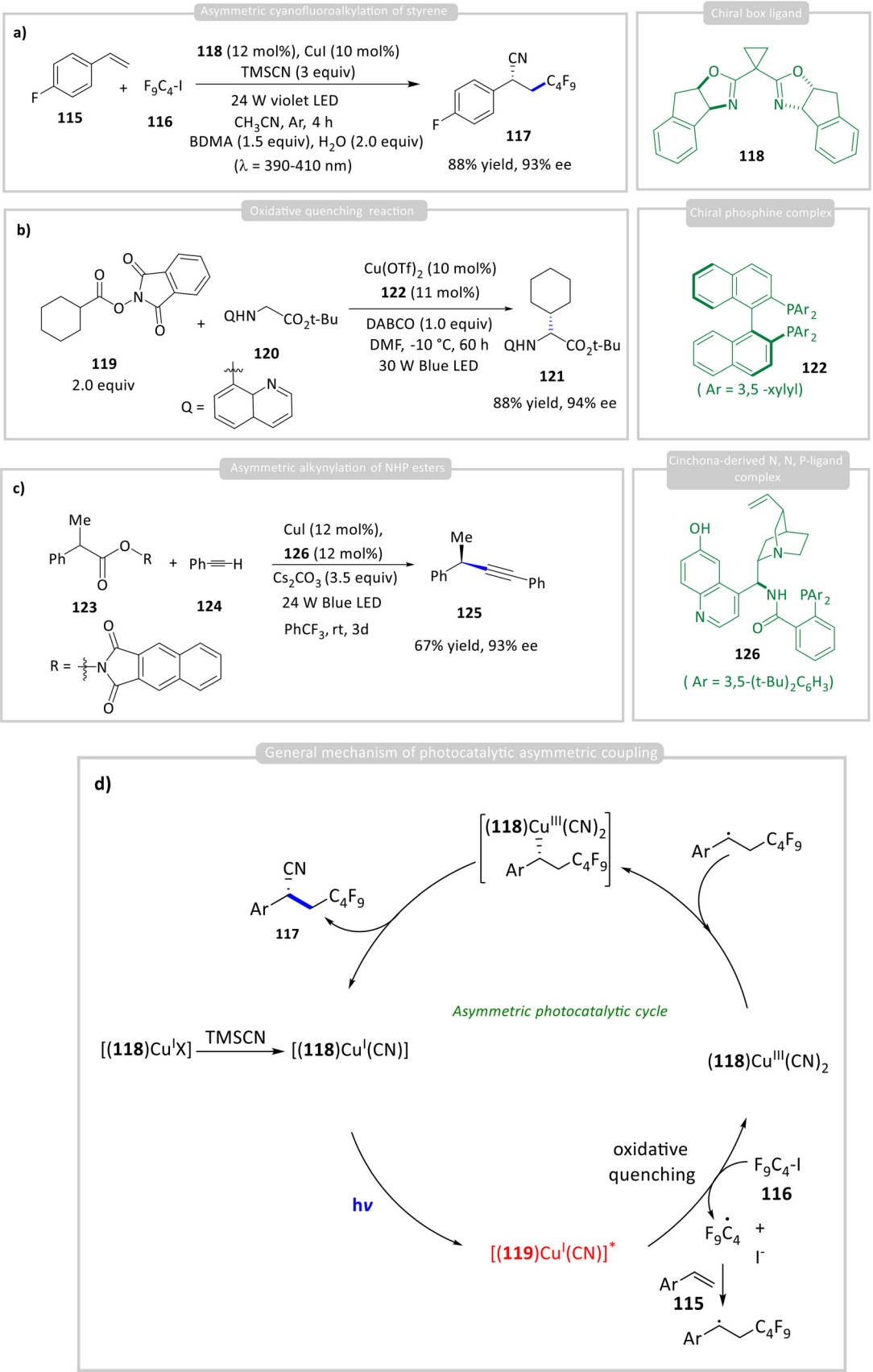

Scheme 12 Photocatalytic asymmetric (a) cyanofluoroalkylation of styrene, (b) oxidative quenching reaction, (c) alkynylation of NHP esters, and (d) general mechanism of coupling reactions with a copper(I) chiral photocatalyst.

across various substrates (Scheme 10a).[49] The reaction proceeds *via* ground-state complexation of **104** with **Λ-107**, followed by photoexcitation and single-electron reduction by **105** to generate the α-amino radical. This radical adds to the metal-bound substrate, forming a secondary radical that undergoes further reduction and protonation to yield product **106**, completing the cycle. In a subsequent study, they applied **Λ-107** to the asymmetric Giese addition of *p*-aminobenzyl radicals derived from carboxylic acids **109** to α,β-unsaturated 2-acylimidazoles **108**, affording product **110** in up to 79% yield and 95% ee under visible light (Scheme 10b).[50]

3.5 Copper-incorporated chiral metal complexes

Copper-based photocatalysts have become popular materials for photoredox catalytic reactions due to their abundance, low cost, and ability to provide strong photoexcited reducing power. Key characteristics of Cu(I) photocatalysts involve the production of radical species through the reduction of organic substrates upon photoexcitation, followed by the capture of the resulting radical and/or anionic species in a rebound process. The transient Cu(III) intermediate formed can undergo reductive elimination to yield cross-coupled products. Alternatively, the Cu(II) intermediate can exchange ligands with the radical to form cross-coupled products.[51]

In the case of chiral photocatalysis, the majority of reported photoactive chiral copper-based photocatalysts involve the use of chiral ligands for the stereocontrol of organic reactions. This is because tetrahedral copper complexes readily undergo fast ligand exchange, which prevents the exploitation of any metal-centred chirality.[52] Bach and co-workers reported the photocatalytic electrocyclization of 6π system **111** using Cu(II)-chiral BOX ligand **113** (Scheme 11).[53] As the substrate co-ordinates

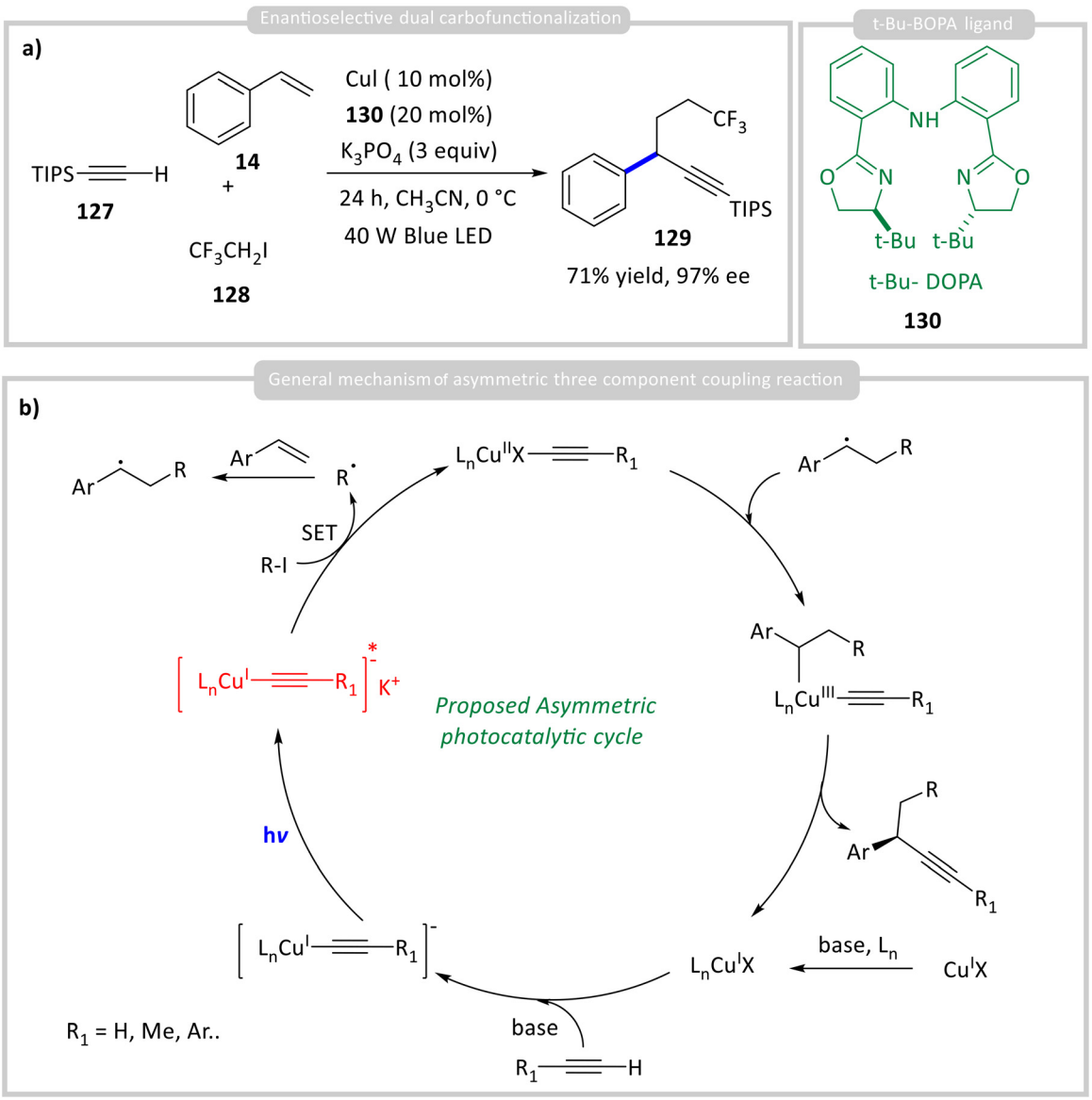

Scheme 13 Photocatalytic asymmetric (a) dual carbofunctionalization reaction and (b) general mechanism.

with the copper centre of the photocatalyst, a bathochromic shift is observed in the absorption spectra of the substrate. Using an *in situ*-generated photocatalyst with 50 mol% of $Cu(ClO_4)\cdot 6H_2O$ and 60 mol% of chiral BOX ligand **113**, they achieved up to 40% ee and 53% yield of the cyclized product **112**.

Xu, Wang, and co-workers later reported a chiral photocatalytic method for the asymmetric cyanofluoroalkylation of styrene **115** using a chiral BOX ligand **118** with CuI (Scheme 12a).[54] The active photocatalyst, an *in situ*-generated complex of the chiral BOX ligand **118** and CuI, exhibited a

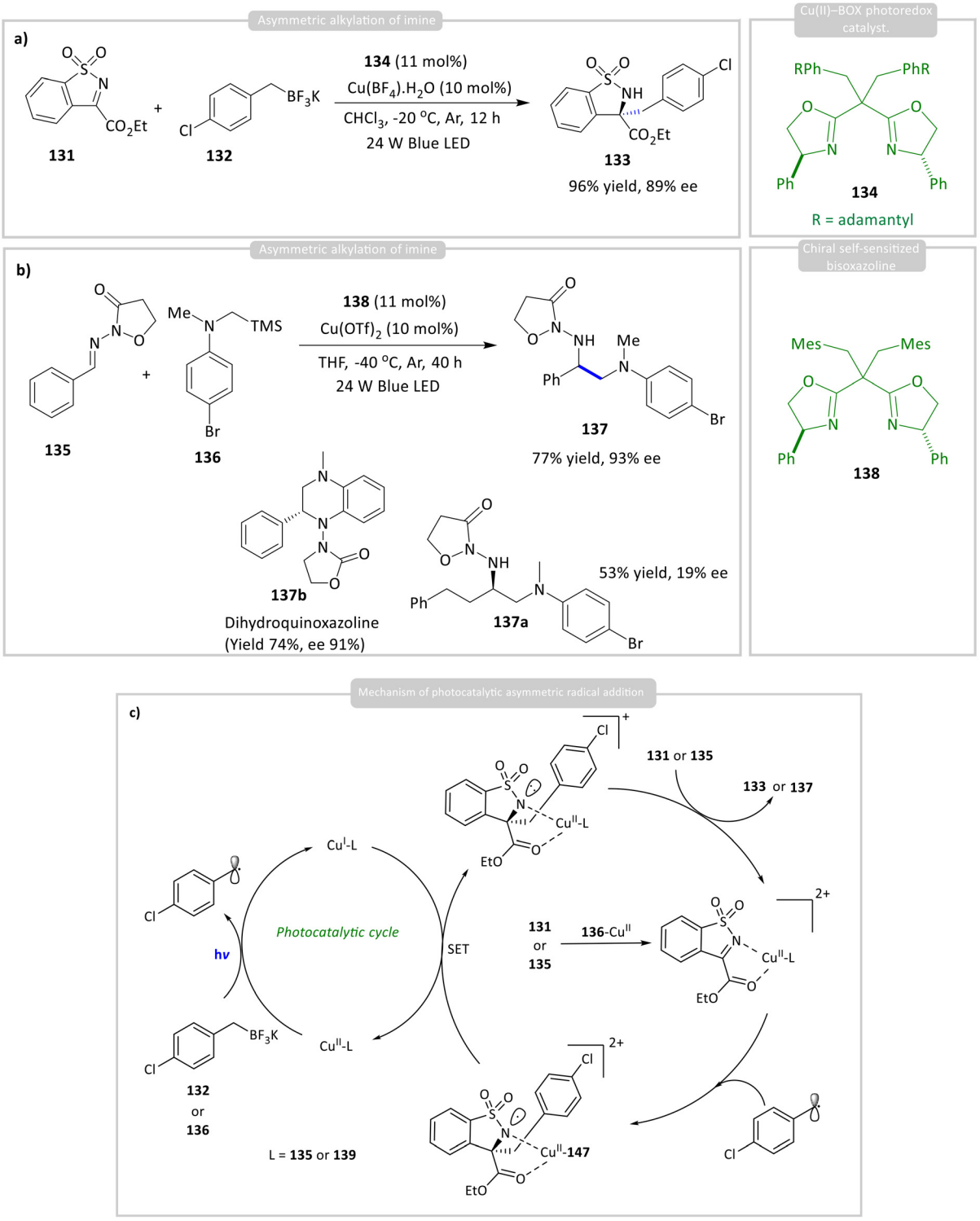

Scheme 14 Photocatalytic asymmetric (a) & (b) alkylation of imines; (c) general mechanism of the reaction using a chiral Cu(I)-BOX photocatalyst.

high reduction potential in its excited state (−2.24 V *vs.* SCE). This allowed for the generation of an alkyl radical from perfluoroalkyl iodide **116** (−1.32 V *vs.* SCE), resulting in the formation of product **117** (Scheme 12d) in 88% yield with 93% enantiomeric excess (ee). Xu and Wang reported the enantioselective C(sp^3)–H alkylation of quinolinyl-appended glycinate ester **119** using NHP ester **120** as the alkyl radical precursor (Scheme 12b).[55] Coordination of **120** to a chiral phosphine-Cu(I) complex generates the photocatalyst *in situ*, while oxidative quenching by **119** furnishes the alkyl radical. The optimized reaction delivered the cross-coupled product **121** in 88% yield and 94% ee. Similarly, Liu developed an asymmetric alkynylation of NHP esters **123** with a Cu(I)-acetylide complex bearing cinchona-derived N,N,P-ligand **126** (Scheme 12c).[56] The use of naphthyl NHP ester **123** was crucial, as it suppressed Glaser homocoupling of alkyne **124** and radical dimerization of **123**, likely by slowing quenching of the excited Cu complex relative to standard NHP esters. Control experiments showed that without ligand **126**, only 10% of product **125** was formed, highlighting the ligand's key role in enhancing photocatalytic efficiency. Unfortunately, the homobenzylic substrates delivered racemic coupling products **125a** & **125b**.

Zhang and co-workers developed another chiral photocatalyst, and this was applied for enantioselective dual carbofunctionalization of styrene derivative **14** (Scheme 13a).[57] From the UV-vis experiments, they observed that the photocatalyst is generated through the aggregation of chiral *t*-Bu-BOPA ligand **130** and a nucleophile from alkyne **126** to form a Cu(I)-acetylide species, leading to the formation of enantioselective products **129** in up to 71% yield with 97% ee (Scheme 13b). The co-ordination of alkyl halide **128** was confirmed by steady-state luminescence quenching studies.

Gong and co-workers developed a Cu(II) complex with ligands **134**/**138** as chiral photocatalysts. This system was used for the photocatalytic asymmetric alkylation of imines **133**/**135** with **132**/**135**, producing enantioselective products **133**/**147** containing tetrasubstituted carbon centres in yields of up to 96% with an enantiomeric excess (ee) of 98% of **134** and 77% yield and 93% ee of **137**, respectively (Scheme 14).[58] The mechanism involves photoexcited ligand-to-metal charge transfer (LMCT), which generates an alkyl radical. This radical then undergoes nucleophilic addition to the coordinated imine substrate, forming a nitrogen-centred radical stabilized by Cu(II), which is subsequently reduced by the Cu(I) complex. It is worth noting that the alkyl-substituted aldimine exhibited low reactivity under the standard reaction conditions. The desired product **137a** was obtained in 73% yield with significantly reduced enantioselectivity (19% ee) at an elevated temperature of 25 °C over 40 h. Furthermore, a bioactive dihydroquinoxazoline **137b** was synthesized in 74% yield with 91% ee *via* a Pd-catalyzed intramolecular cross-coupling reaction of the corresponding enantiopure intermediate.

In a subsequent study, Gong and co-workers applied the same strategy to the asymmetric cross-coupling of 2-acylimidazole **139** with xanthene derivatives **140**, using O_2 as the terminal oxidant to afford product **141** in up to 71% yield and 92% ee (Scheme 15).[59] Mechanistic insights from electrochemical and spectroscopic studies revealed that the chiral photocatalyst, a Cu(II)–BOX complex formed from $Cu(BF_4)_2{\cdot}H_2O$ and chiral ligand **142**, initiates the reaction through oxidation

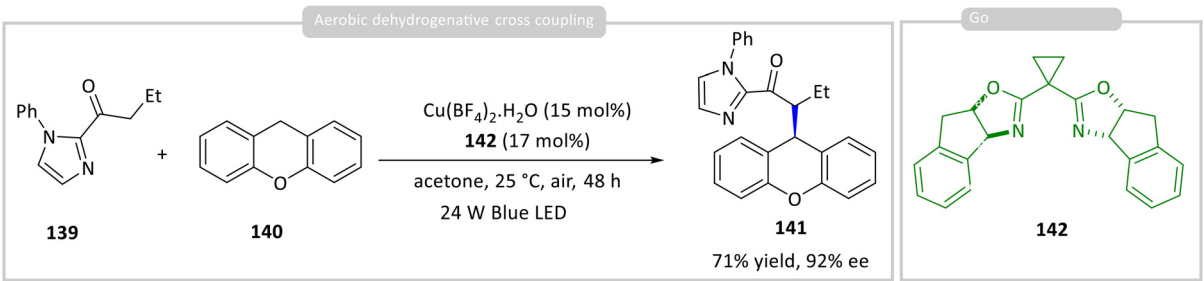

Scheme 15 Photocatalytic asymmetric aerobic dehydrogenative cross-coupling.

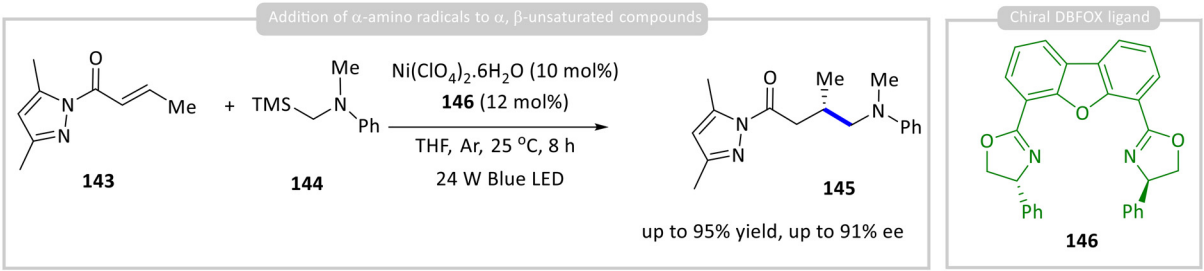

Scheme 16 Photocatalytic asymmetric addition of α-amino radicals to α,β-unsaturated carbonyl compounds.

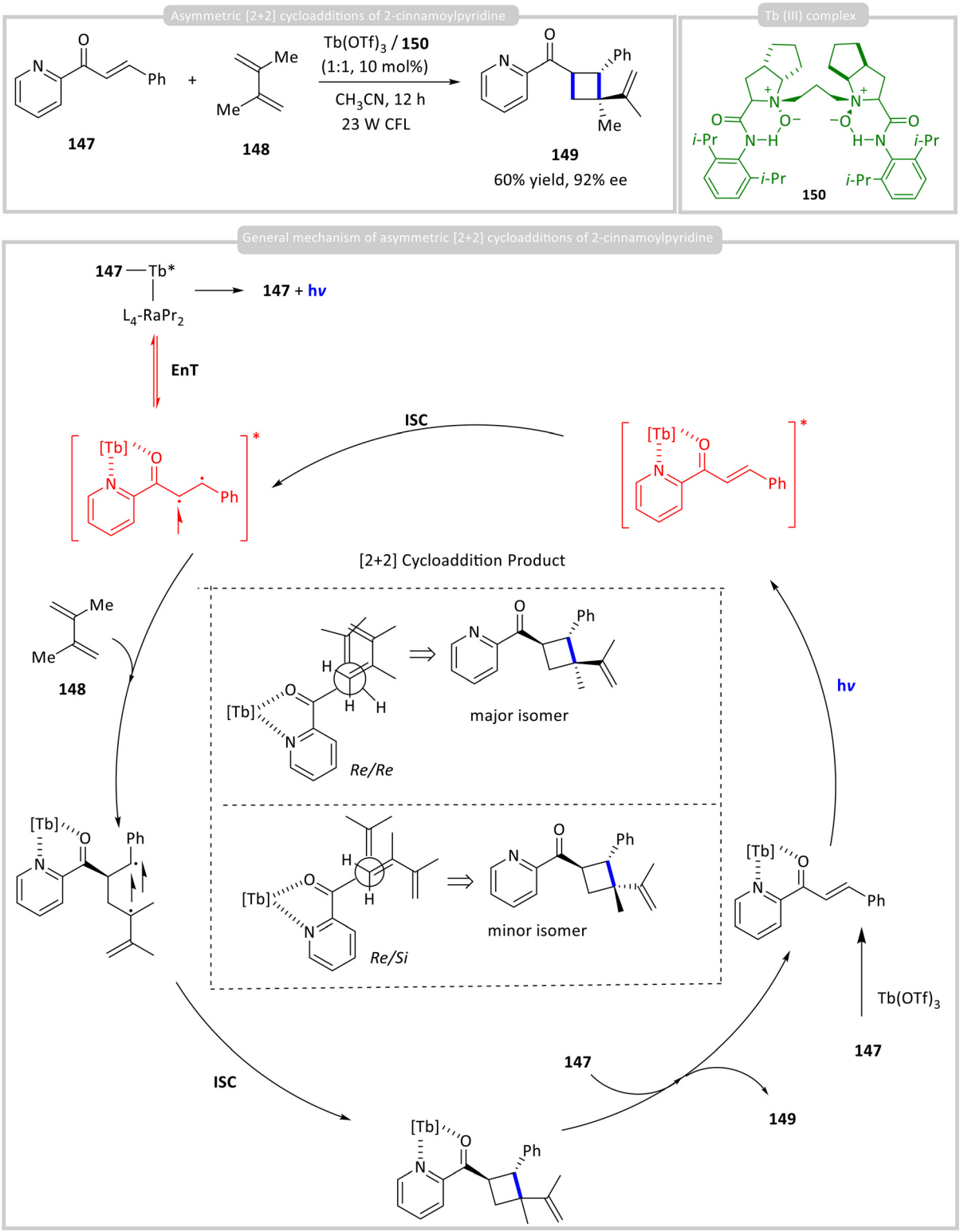

Scheme 17 Photocatalytic asymmetric [2 + 2] cycloaddition of 2-cinnamoylpyridine with dialkenes.

of xanthene **140**. Moreover, binding of the prochiral substrate **139** by the Cu(II)–BOX complex provides the chiral environment necessary for enantioinduction for the synthesis of **141**.

3.6 Nickel-incorporated chiral metal complexes

Shen and co-workers developed a bifunctional Ni(II)–DBFOX complex, prepared from $Ni(ClO_4)_2 \cdot 6H_2O$ and the chiral DBFOX

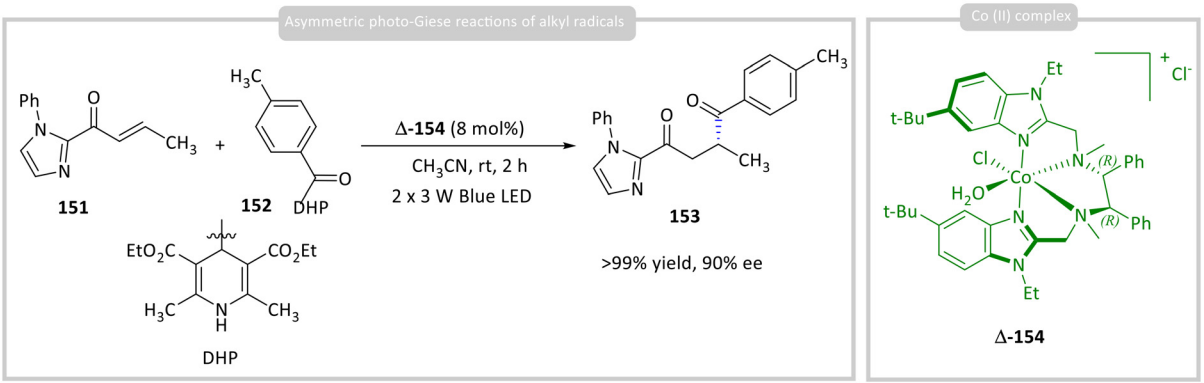

Scheme 18 Photocatalytic asymmetric photo-Giese reactions of alkyl radicals using a chiral Co(II) photocatalyst.

ligand **146**. This complex acts simultaneously as a photoredox catalyst and a chiral Lewis acid, enabling the asymmetric addition of α-amino radicals derived from **144** to α,β-unsaturated compounds **143**, a de-silylative photo-oxidation pathway that generates the key α-amino radical intermediate, affording product **145** (Scheme 16).[60]

3.7 Lanthanide-incorporated chiral metal complexes

Only a limited number of chiral photocatalysts based on lanthanide coordination complexes have been reported for asymmetric photocatalytic carbon–carbon bond-forming reactions. Liu, Feng, and co-workers developed such a system using a chiral Tb(III) complex, prepared from $Tb(OTf)_3$ and chiral ligand **150**, as a chiral photocatalyst for the asymmetric [2 + 2] cycloaddition of 2-cinnamoylpyridine **147** with dialkene **148**. This method delivered cycloadduct **149** in up to 92% enantiomeric excess (ee) and 60% yield (Scheme 17).[61] The formation of the chiral Tb(III) complex was confirmed by UV-vis absorption spectroscopy. The heavy-atom effect of Tb(III) promotes intersystem crossing (ISC), enabling efficient harvesting of the triplet state and driving the bimolecular reaction under photoexcitation. Single-crystal X-ray analysis of the *in situ*-generated metal complex revealed an eight-coordinate, square-antiprismatic geometry. The proposed mechanism involves pre-association of the chiral Tb(III) complex with substrate **147** in the ground state, followed by excitation. After intersystem crossing, substrate **148** replaces product **149** in the coordination sphere, thereby completing the catalytic cycle.

3.8 Cobalt-incorporated chiral metal complexes

Lu, Xiao, and co-workers reported the development of a chiral octahedral cobalt(II) complex **Δ-154** from Earth-abundant cobalt(II) and bisoxazoline-type (BOX-like) *N*,*N*-bidentate chelating N_4 ligands. The chiral Co(II) complex **Δ-154** was demonstrated to function as a highly efficient catalyst for visible-light-induced conjugate addition reactions. Enone **151** undergoes asymmetric addition with acyl radicals that are generated *in situ* from the corresponding Hantzsch esters **152**. The catalytic cycle proceeds under visible-light irradiation, where the Co(II) complex **Δ-154** not only enables photoredox activation but also imparts stereocontrol through its chiral coordination environment to obtain enantioselective 1,4-dicarbonyl product **153** in >99% yields with 90% ee (Scheme 18).[62]

4. Summary and outlook

The field of chiral photocatalysis has witnessed remarkable growth in recent years, particularly in enabling asymmetric carbon–carbon (C–C) bond-forming reactions under mild and sustainable conditions. These catalysts control their well-defined chiral environments to promote stereo-controlled C–C bond formation under mild photochemical conditions, reducing dependence on harsh reagents or elaborate reaction setups. Although many chiral photocatalysts were initially designed for thermal asymmetric transformations, their successful application in excited-state photocatalytic reactions has demonstrated remarkable control over stereochemistry, particularly in C–C bond-forming processes.

After these breakthroughs, a variety of chiral photocatalytic systems incorporating chromophores or chiral ligands have been developed specifically for reactions that are challenging or inaccessible with ground-state catalysis. Notably, Bach's and Meggers' groups have made significant contributions through the development of chiral organo-photocatalysts and chiral-at-metal complexes, which act as photoactive chiral molecules in enantioselective C–C bond-forming reactions. In parallel, other strategies have employed dual catalysts, where a chiral catalyst is attached to a photocatalyst to guide asymmetric induction during C–C coupling. Yoon's group has also advanced the field with hydrogen-bonding chiral-at-metal photocatalysts, enabling highly stereoselective cycloadditions and related C–C bond formations. Despite differences in mechanistic pathways and structural designs, a key aspect underlying successful enantioselective C–C bond formation is the pre-association of substrates with the chiral catalyst in the ground state, which facilitates chiral induction upon photoexcitation and helps suppress racemic background reactions. The continued evolution of photoactive chiral systems has massively expanded the synthetic approaches for constructing

complex, enantioselective carbon frameworks. As the field advances, chiral photocatalysts are expected to remain central to the development of selective and scalable synthetic methods for asymmetric C–C bond formation.

In terms of atom economy and reaction efficiency, both organic and metal-based photocatalysts effectively promote bond formation under light irradiation. Organic photocatalysts often provide high selectivity with minimal side reactions. In contrast, metal-based photocatalysts, particularly transition-metal complexes, though relatively expensive, possess well-defined redox properties and efficiently mediate single-electron transfer processes, enabling a broad substrate scope and high enantioselectivity in asymmetric transformations. From a sustainability perspective, organic photocatalysts are generally considered more environmentally benign due to their metal-free nature, lower toxicity, and compatibility with visible light and green solvents. Regarding practical implementation and scalability, organic photocatalysts typically operate under mild conditions, improving energy efficiency and reducing operational costs. While metal-based systems offer superior catalytic control, challenges associated with catalyst recovery and recycling may limit their industrial applicability. In this context, metal-free and immobilized catalytic systems, such as those based on chiral COFs, offer advantages in recyclability and simplified purification, making them attractive for scalable processes.

Future efforts will focus on enhancing yields, enantiomeric excess (ee), and operational stability, with particular emphasis on designing robust, tuneable photocatalysts capable of long-term use under visible light. These developments will be critical for enabling industrial-scale applications, especially in pharmaceutical synthesis, where precise control over stereochemistry is essential. Moreover, chiral photocatalysts are anticipated to impact materials science, facilitating the creation of enantioselective polymers and chiral surfaces for use in sensors, optoelectronics, and other advanced technologies. Improving photocatalyst stability and resistance to photodegradation will be crucial for unlocking the full potential of asymmetric C–C bond formation in photocatalytic systems.

Author contributions

AD planned, designed and overall supervised this review article. VKS and AHI gathered references and prepared the schemes and structures.

Conflicts of interest

The authors declare no conflict of interest.

Data availability

No primary research results, software or code have been included, and no new data were generated or analysed as part of this review.

Acknowledgements

VKS and AHI gratefully acknowledge the Department of Chemistry, SRM Institute of Science and Technology, Kattankulathur, Tamil Nadu, India, for financial support through an Institute Doctoral Fellowship. AD sincerely acknowledges SRMIST for the seed grant (no. SRMIST/R/AR(A/SERI2024/174/14-342)), the Anusandhan National Research Foundation (ANRF-ECRG, Grant No. ANRF/ECRG/2024/003299/CS), and the Royal Society-Newton International Alumni Fellowship (AL\24100051) for financial support.

References

1 (*a*) E. J. Corey and X.-M. Cheng, *The Logic of Chemical Synthesis*, John Wiley & Sons, New York, 1989; (*b*) D. Ravelli, S. Protti and M. Fagnoni, *Chem. Rev.*, 2016, **116**, 9850–9913; (*c*) V. Saini, B. J. Stokes and M. S. Sigman, *Angew. Chem., Int. Ed.*, 2013, **52**, 11206–11220; (*d*) N. G. Schmidt, E. Eger and W. Kroutil, *ACS Catal.*, 2016, **6**, 4286–4311; (*e*) S. Van de Vyver and Y. Roman-Leshkov, *Angew. Chem., Int. Ed.*, 2015, **54**, 12554–12561; (*f*) Q. Liu, R. Jackstell and M. Beller, *Angew. Chem., Int. Ed.*, 2013, **52**, 13871–13873; (*g*) T. Tsubogo, T. Ishiwata and S. Kobayashi, *Angew. Chem., Int. Ed.*, 2013, **52**, 6590–6604; (*h*) H. Schönherr and T. Cernak, *Angew. Chem., Int. Ed.*, 2013, **52**, 12256–12267; (*i*) S. H. Cho, J. Y. Kim, J. Kwak and S. Chang, *Chem. Soc. Rev.*, 2011, **40**, 5068–5083; (*j*) F. Monnier and M. Taillefer, *Angew. Chem., Int. Ed.*, 2009, **48**, 6954–6971; (*k*) A. Alexakis, J.-E. Bäckvall, N. Krause, O. Pàmies and M. Diéguez, *Chem. Rev.*, 2008, **108**, 2796–2823; (*l*) B. M. Trost, F. D. Toste and A. B. Pinkerton, *Chem. Rev.*, 2001, **101**, 2067–2096; (*m*) N. Miyaura and A. Suzuki, *Chem. Rev.*, 1995, **95**, 2457–2483; (*n*) R. Franzén, *Can. J. Chem.*, 2000, **78**, 957–962; (*o*) R. Franzén and Y. Xu, *Can. J. Chem.*, 2005, **83**, 266–272; (*p*) L. Yin and J. Liebscher, *Chem. Rev.*, 2006, **107**, 133–173; (*q*) J. Barluenga, M. Tomás-Gamasa, F. Aznar and C. Valdés, *Nat. Chem.*, 2009, **1**, 494–499; (*r*) P. Clapés, W.-D. Fessner, G. A. Sprenger and A. K. Samland, *Curr. Opin. Chem. Biol.*, 2010, **14**, 154–167; (*s*) D. G. Gillingham, P. Stallforth, A. Adibekian, P. H. Seeberger and D. Hilvert, *Nat. Chem.*, 2010, **2**, 102–105; (*t*) J. Soloducho, J. Cabaj, K. Idzik, A. Nowakowska-Oleksy, A. Swist and M. Lapkowski, *Curr. Org. Chem.*, 2010, **14**, 1234–1245; (*u*) V. Resch, J. H. Schrittwieser, E. Siirola and W. Kroutil, *Curr. Opin. Biotechnol.*, 2011, **22**, 793–799; (*v*) M. Pérez, M. Fañanás-Mastral, P. H. Bos, A. Rudolph, S. R. Harutyunyan and B. L. Feringa, *Nat. Chem.*, 2011, **3**, 377–381; (*w*) A. Bhunia, R. S. Yetra and A. T. Biju, *Chem. Soc. Rev.*, 2012, **41**, 3140–3152; (*x*) G. Brahmachari, *Chem. Rec.*, 2016, **16**, 98–123.

2 (*a*) E. Negishi, *Angew. Chem., Int. Ed.*, 2011, **50**, 6738–6764; (*b*) C. C. C. Johansson Seechurn, M. O. Kitching, T. J. Colacot and V. Snieckus, *Angew. Chem., Int. Ed.*, 2012, **51**, 5062–5085; (*c*) A. H. Cherney, N. T. Kadunce and S. E. Reisman, *Chem. Rev.*, 2015, **115**, 9587–9652;

(*d*) K. Faber, W.-D. Fessner and N. J. Turner, Biocatalysis in Organic Synthesis, in *Science of Synthesis*, Georg Thieme, Stuttgart, 2015, vol. 1–3; (*e*) H. Lechner, D. Pressnitz and W. Kroutil, *Biotechnol. Adv.*, 2015, **33**, 457–480; (*f*) Y.-F. Miao, M. Rahimi, E. M. Geertsema and G. J. Poelarends, *Curr. Opin. Chem. Biol.*, 2015, **25**, 115–123; (*g*) L. A. Wessjohann, J. Keim, B. Weigel and M. Dippe, *Curr. Opin. Chem. Biol.*, 2013, **17**, 229–235; (*h*) K. Fesko and M. Gruber-Khadjawi, *ChemCatChem*, 2013, **5**, 1248–1272; (*i*) M. Müller, *Adv. Synth. Catal.*, 2012, **354**, 3161–3174; (*j*) K. Faber, *Biotransformations in Organic Chemistry*, Springer, Heidelberg, 6th edn, 2011; (*k*) M. Brovetto, D. Gamenara, P. S. Mendez and G. A. Seoane, *Chem. Rev.*, 2011, **111**, 4346–4403; (*l*) G. Brahmachari, *RSC Adv.*, 2016, **6**, 64676–64725.

3 (*a*) C. K. Prier, D. A. Rankic and D. W. C. MacMillan, *Chem. Rev.*, 2013, **113**, 5322–5363; (*b*) D. Staveness, I. Bosque and C. R. J. Stephenson, *Acc. Chem. Res.*, 2016, **49**, 2295–2306; (*c*) F. Strieth-Kalthoff, M. J. James, M. Teders, L. Pitzera and F. Glorius, *Chem. Soc. Rev.*, 2018, **47**, 7190–7202; (*d*) J. Xuan and W.-J. Xiao, *Angew. Chem., Int. Ed.*, 2012, **51**, 6828–6838; (*e*) L. Shi and W. Xia, *Chem. Soc. Rev.*, 2012, **41**, 7687–7697; (*f*) G. Ciamician, *Science*, 1912, **36**, 385–394; (*g*) H. D. Roth, *Angew. Chem., Int. Ed. Engl.*, 1989, **28**, 1193–1207; (*h*) Y. Inoue and V. Ramamurthy, *Chiral Photochemistry*, Marcel Dekker, 2004, vol. 11; (*i*) A. Das, T. Banerjee and K. Hanson, *Chem. Commun.*, 2016, **52**, 1350–1353; (*j*) *Visible Light Photocatalysis in Organic Chemistry*, ed. C. R. J. Stephenson, D. W. C. MacMillan and T. P. Yoon, Wiley-VCH, Weinheim, 2018; (*k*) M. H. Shaw, J. Twilton and D. W. C. MacMillan, *J. Org. Chem.*, 2016, **81**, 6898–6926; (*l*) V. Ramamurthy and J. Sivaguru, *Chem. Rev.*, 2016, **116**, 9914–9993; (*m*) F. Mohamadpour and A. M. Amani, *RSC Adv.*, 2024, **14**, 20609–20615; (*n*) A. Albini and M. Fagnoni, *Green Chem.*, 2004, **6**, 1–6; (*o*) N. Hoffmann, *Chem. Rev.*, 2008, **108**, 1052–1103; (*p*) A. Houmam, *Chem. Rev.*, 2008, **108**, 2180–2237; (*q*) J. M. R. Narayanam and C. R. J. Stephenson, *Chem. Soc. Rev.*, 2011, **40**, 102–113; (*r*) D. M. Schultz and T. P. Yoon, *Science*, 2014, **343**, 1239176; (*s*) N. A. Romero and D. A. Nicewicz, *Chem. Rev.*, 2016, **116**, 10075–10166; (*t*) K. L. Skubi, T. R. Blum and T. P. Yoon, *Chem. Rev.*, 2016, **116**, 10035–10074; (*u*) J. Twilton, C. Le, P. Zhang, M. H. Shaw, R. W. Evans and D. W. C. MacMillan, *Nat. Rev. Chem.*, 2017, **1**, 0052; (*v*) J. K. Matsui, S. B. Lang, D. R. Heitz and G. A. Molander, *ACS Catal.*, 2017, **7**, 2563–2575; (*w*) P. Chuentragool, D. Kurandina and V. Gevorgyan, *Angew. Chem., Int. Ed.*, 2019, **58**, 11586–11590; (*x*) R. Kancherla, K. Muralirajan, S. Arunachalam and M. Rueping, *Trends Chem.*, 2019, **1**, 510–523; (*y*) D. Kurandina, P. Chuentragool and V. Gevorgyan, *Synthesis*, 2019, 985–999; (*z*) W.-J. Zhou, G.-M. Cao, Z.-P. Zhang and D.-G. Yu, *Chem. Lett.*, 2019, **48**, 181–184.

4 (*a*) Y. Inoue, *Chem. Rev.*, 1992, **92**, 741–770; (*b*) R. Brimioulle, D. Lenhart, M. M. Maturi and T. Bach, *Angew. Chem., Int. Ed.*, 2015, **54**, 3872–3890; (*c*) B. S. Green, A. T. Hagler, Y. Rabinsohn and M. Rejtő, *Isr. J. Chem.*, 1976, **15**, 124–130; (*d*) L. M. Tolbert and M. B. Ali, *J. Am. Chem. Soc.*, 1982, **104**, 1742–1744; (*e*) A. Joy, J. R. Scheffer and V. Ramamurthy, *Org. Lett.*, 2000, **2**, 119–121; (*f*) M. Nishijima, T. Wada, T. Mori, T. C. S. Pace, C. Bohne and Y. Inoue, *J. Am. Chem. Soc.*, 2007, **129**, 3478–3479; (*g*) L. Addadi, J. V. Mil and M. Lahav, *J. Am. Chem. Soc.*, 1982, **104**, 3422–3429; (*h*) S. V. Evans, M. G. Garibay, N. Omkaram, J. R. Scheffer, J. Trotter and F. Wireko, *J. Am. Chem. Soc.*, 1986, **108**, 5648–5650; (*i*) A. Das, S. Ayad and K. Hanson, *Org. Lett.*, 2016, **18**, 5416–5419; (*j*) Y. Li, Z. Huangfu, Y. Li, X. Song, Y. Duan, Y. Zhang and X. Li, *ACS Catal.*, 2025, **15**, 7543–7577.

5 (*a*) Y. Wang, E. A. Bazan-Bergamino and M.-Y. Ngai, *ChemCatChem*, 2022, **14**, e202101292; (*b*) C. Wang and Z. Lu, *Org. Chem. Front.*, 2015, **2**, 179–190; (*c*) A. F. Garrido-Castro, M. C. Maestro and J. Alemán, *Tetrahedron Lett.*, 2018, **59**, 1286–1289; (*d*) M. Silvi and P. Melchiorre, *Nature*, 2018, **554**, 41–49; (*e*) Y.-Q. Zou, F. M. Hoermann and T. Bach, *Chem. Soc. Rev.*, 2018, **47**, 278–290; (*f*) X. Jiang, X. Han, F.-D. Lu, L.-Q. Lu, Z. Zuo and W.-J. Xiao, *CCS Chem.*, 2025, **7**, 1567–1602.

6 (*a*) S. J. Chapman, W. B. Swords, C. M. Le, I. A. Guzei, F. D. Toste and T. P. Yoon, *J. Am. Chem. Soc.*, 2022, **144**, 4206–4213; (*b*) Z. Zuo, H. Cong, W. Li, J. Choi, G. C. Fu and D. W. C. MacMillan, *J. Am. Chem. Soc.*, 2016, **138**, 1832–1835; (*c*) E. R. Welin, A. A. Warkentin, J. C. Conrad and D. W. C. MacMillan, *Angew. Chem., Int. Ed.*, 2015, **54**, 9668–9672; (*d*) J. A. Terrett, M. D. Clift and D. W. C. MacMillan, *J. Am. Chem. Soc.*, 2014, **136**, 6858–6861; (*e*) S. Qian, T. M. Lazarus and D. A. Nicewicz, *J. Am. Chem. Soc.*, 2023, **145**, 18247–18252; (*f*) J. B. McManus, J. D. Griffin, A. R. White and D. A. Nicewicz, *J. Am. Chem. Soc.*, 2020, **142**, 103; (*g*) C. Prentice, J. Morrisson, A. D. Smith and E. Zysman-Colman, *Beilstein J. Org. Chem.*, 2020, **16**, 2363–2441; (*h*) Y. Li, Z. Huangfu, Y. Li, X. Song, Y. Duan, Y. Zhang and X. Li, *ACS Catal.*, 2025, **15**, 7543–7577; (*i*) B.-C. Hong, *Org. Biomol. Chem.*, 2020, **18**, 4298–4353; (*j*) C. Jiang, W. Chen, W.-H. Zheng and H. Lu, *Org. Biomol. Chem.*, 2019, **17**, 8673–8689.

7 (*a*) A. J. David, R. Balaji and A. Das, *Adv. Synth. Catal.*, 2025, **367**, e202401543; (*b*) E. Studer, S. Mandal, T. Stünkel and R. Gilmour, *Angew. Chem., Int. Ed.*, 2025, **64**, e202513320; (*c*) M. J. Genzink, J. B. Kidd, W. B. Swords and T. P. Yoon, *Chem. Rev.*, 2022, **122**, 1654–1716; (*d*) J. Soika, C. Onneken, T. Morack and R. Gilmour, *Acc. Chem. Res.*, 2025, **58**, 1710–1723.

8 (*a*) G. E. M. Crisenza, D. Mazzarella and P. Melchiorre, *J. Am. Chem. Soc.*, 2020, **142**, 5461–5476; (*b*) C. G. S. Lima, T. M. Lima, M. Duarte, I. D. Jurberg and M. W. Paixão, *ACS Catal.*, 2016, **6**, 1389–1407.

9 (*a*) W. Ding, L.-Q. Lu, Q.-Q. Zhou, Y. Wei, J.-R. Chen and W.-J. Xiao, *J. Am. Chem. Soc.*, 2017, **139**, 63–66; (*b*) A. B. Rolka, N. Archipowa, R. J. Kutta, B. König and F. D. Toste, *J. Org. Chem.*, 2023, **88**, 6509–6522; (*c*) Y. Zhang, Y. Sun, X. Ren, J. Hu, H. Yu, J. Liu, H. Huang and J. Han,

Angew. Chem., Int. Ed., 2025, **64**, e202416221; (*d*) B.-J. Bian, L. Yang, L.-X. Qiao, Q. Zhang and W. He, *RSC Adv.*, 2025, **15**, 2874–2880; (*e*) J. Lyu, M. Leone, A. Claraz, C. Allain, L. Neuville and G. Masson, *RSC Adv.*, 2021, **11**, 36663–36669; (*f*) A. B. Rolka and B. König, *Nat. Synth.*, 2023, **2**, 913–925.

10 C. Jiang, W. Chen, W.-H. Zheng and H. Lu, *Org. Biomol. Chem.*, 2019, **17**, 8673–8689.

11 (*a*) N. Holmberg-Douglas, Y. Choi, B. Aquila, H. Huynh and D. A. Nicewicz, *ACS Catal.*, 2021, **11**, 3153–3158; (*b*) V. A. Pistritto, M. E. Schutzbach-Horton and D. A. Nicewicz, *J. Am. Chem. Soc.*, 2020, **142**, 17187–17194.

12 (*a*) R. Maeda, T. Wada, T. Mori, S. Kono, N. Kanomata and Y. Inoue, *J. Am. Chem. Soc.*, 2011, **133**, 10379–10381; (*b*) R. Hoffmann and Y. Inoue, *J. Am. Chem. Soc.*, 1999, **121**, 10702–10710; (*c*) Y. Inoue, H. Shimoyama, N. Yamasaki and A. Tai, *Chem. Lett.*, 1991, **20**, 593–596; (*d*) Y. Inoue, N. Yamasaki, H. Shimoyama and A. Tai, *J. Org. Chem.*, 1993, **58**, 1785–1793.

13 J.-I. Kim and G. B. Schuster, *J. Am. Chem. Soc.*, 1990, **112**, 9635–9637.

14 (*a*) T. Bach, H. Bergmann and K. Harms, *Angew. Chem., Int. Ed.*, 2000, **39**, 2302–2304; (*b*) T. Bach, H. Bergmann, B. Grosch, K. Harms and E. Herdtweck, *Synthesis*, 2001, 1395–1405.

15 C. Müller, A. Bauer and T. Bach, *Angew. Chem., Int. Ed.*, 2009, **48**, 6640–6642.

16 (*a*) A. Bauer, F. Westkämper, S. Grimme and T. Bach, *Nature*, 2005, **436**, 1139–1140; (*b*) Y. Inoue, *Nature*, 2005, **436**, 1099–1100.

17 X. Li, J. Großkopf, C. Jandl and T. Bach, *Angew. Chem., Int. Ed.*, 2021, **60**, 2684–2688.

18 A. Tröster, R. Alonso, A. Bauer and T. Bach, *J. Am. Chem. Soc.*, 2016, **138**, 7808–7811.

19 M. M. Maturi and T. Bach, *Angew. Chem., Int. Ed.*, 2014, **53**, 7661–7664.

20 F. Pecho, Y.-Q. Zou, J. Gramüller, T. Mori, S. M. Huber, A. Bauer, R. M. Gschwind and T. Bach, *Chem. – Eur. J.*, 2020, **26**, 5190–5194.

21 F. Pecho, Y. Sempere, J. Gramüller, F. M. Hörmann, R. M. Gschwind and T. Bach, *J. Am. Chem. Soc.*, 2021, **143**, 9350–9354.

22 E. Arceo, I. D. Jurberg, Á. Álvarez-Fernández and P. Melchiorre, *Nat. Chem.*, 2013, **5**, 750–756.

23 M. Silvi, E. Arceo, I. D. Jurberg, C. Cassani and P. Melchiorre, *J. Am. Chem. Soc.*, 2015, **137**, 6120–6123.

24 T. Rigotti, A. Casado-Sánchez, S. Cabrera, R. Pérez-Ruiz, M. Liras, V. A. de la Peña O'Shea and J. Alemán, *ACS Catal.*, 2018, **8**, 5928–5940.

25 E. Arceo, A. Bahamonde, G. Bergonzini and P. Melchiorre, *Chem. Sci.*, 2014, **5**, 2438–2442.

26 Z.-Y. Cao, T. Ghosh and P. Melchiorre, *Nat. Commun.*, 2018, **9**, 3274.

27 D. Mazzarella, G. E. M. Crisenza and P. Melchiorre, *J. Am. Chem. Soc.*, 2018, **140**, 8439–8443.

28 A. M. Nicholas and D. R. Arnold, *Can. J. Chem.*, 1982, **60**, 2165–2179.

29 (*a*) A. G. Amador and T. P. Yoon, *Angew. Chem., Int. Ed.*, 2016, **55**, 2304–2306.

30 (*a*) L. Gong, L.-A. Chen and E. Meggers, *Angew. Chem., Int. Ed.*, 2014, **53**, 10865–10874; (*b*) L. Zhang and E. Meggers, *Chem. – Asian J.*, 2017, **12**, 2335–2342.

31 (*a*) E. Meggers, *Chem. – Eur. J.*, 2010, **16**, 752–758; (*b*) J. Ma, X. Zhang, X. Huang, S. Luo and E. Meggers, *Nat. Protoc.*, 2018, **13**, 605–632.

32 (*a*) A. Werner, *Ber. Dtsch. Chem. Ges.*, 1911, **44**, 1887–1898; (*b*) S. Herrero and M. A. Usón, *J. Chem. Educ.*, 1995, **72**, 1065; (*c*) Y. Zhang, H. Han, Z. Wei, M. Zulqarnain, T. Chang, Y.-S. Chen and E. V. Dikarev, *Inorg. Chem.*, 2025, **64**, 13318–13328.

33 H. Huo, X. Shen, C. Wang, L. Zhang, P. Röse, L. A. Chen, K. Harms, M. Marsch, G. Hilt and E. Meggers, *Nature*, 2014, **515**, 100–103.

34 H. Huo, X. Huang, X. Shen, K. Harms and E. Meggers, *Synlett*, 2016, 749–753.

35 C. Wang, Y. Zheng, H. Huo, P. Röse, L. Zhang, K. Harms, G. Hilt and E. Meggers, *Chem. – Eur. J.*, 2015, **21**, 7355–7359.

36 Y. Tan, W. Yuan, L. Gong and E. Meggers, *Angew. Chem., Int. Ed.*, 2015, **54**, 13045–13048.

37 F. F. de Assis, X. Huang, M. Akiyama, R. A. Pilli and E. Meggers, *J. Org. Chem.*, 2018, **83**, 10922–10932.

38 Z. Zhou, X. Nie, K. Harms, R. Riedel, L. Zhang and E. Meggers, *Sci. China: Chem.*, 2019, **62**, 1512–1518.

39 X. Huang, J. Lin, T. Shen, K. Harms, M. Marchini, P. Ceroni and E. Meggers, *Angew. Chem., Int. Ed.*, 2018, **57**, 5454–5458.

40 K. L. Skubi, J. B. Kidd, H. Jung, I. A. Guzei, M. H. Baik and T. P. Yoon, *J. Am. Chem. Soc.*, 2017, **139**, 17186–17192.

41 J. Zheng, W. B. Swords, H. Jung, K. L. Skubi, J. B. Kidd, G. J. Meyer, M. H. Baik and T. P. Yoon, *J. Am. Chem. Soc.*, 2019, **141**, 13625–13634.

42 W. B. Swords, H. Lee, Y. Park, F. Llamas, K. L. Skubi, J. Park, I. A. Guzei, M.-H. Baik and T. P. Yoon, *J. Am. Chem. Soc.*, 2023, **145**, 27045–27053.

43 A. Böhm and T. Bach, *Synlett*, 2016, 1056–1060.

44 A. Gualandi, F. Calogero, A. Martinelli, A. Quintavalla, M. Marchini, P. Ceroni, M. Lombardo and P. G. Cozzi, *Dalton Trans.*, 2020, **49**, 14497–14505.

45 T. Hamada, H. Ishida, S. Usui, Y. Watanabe, K. Tsumura and K. Ohkubo, *J. Chem. Soc., Chem. Commun.*, 1993, 909–911.

46 T. Hamada, H. Ishida, S. Usui, K. Tsumura and K. Ohkubo, *J. Mol. Catal.*, 1994, **88**, L1–L5.

47 Y. Kimura, D. Uraguchi and T. Ooi, *Org. Biomol. Chem.*, 2021, **19**, 1744–1747.

48 G. E. M. Crisenza, A. Faraone, E. Gandolfo, D. Mazzarella and P. Melchiorre, *Nat. Chem.*, 2021, **13**, 575–580.

49 S. X. Lin, G. J. Sun and Q. A. Kang, *Chem. Commun.*, 2017, **53**, 7665–7668.

50 L. Chen, H. Liangjian, D. Yu, S. Weiping and K. Qiang, *Chin. J. Org. Chem.*, 2020, **40**, 3944–3952.

51 (*a*) A. Reichle and O. Reiser, *Chem. Sci.*, 2023, **14**, 4449; (*b*) A. Hossain, A. Bhattacharyya and O. Reiser, *Science*, 2019, **364**, eaav9713; (*c*) M. Zhong, X. Pannecoucke, P. Jubault and T. Poisson, *Beilstein J. Org. Chem.*, 2020, **16**, 451–481; (*d*) Y. Zhang, Q. Wang, Z. Yan, D. Ma and Y. Zheng, *Beilstein J. Org. Chem.*, 2021, **17**, 2520–2542.

52 K. Endo, Y. Liu, H. Ube, K. Nagata and M. Shionoya, *Nat. Commun.*, 2020, **11**, 6263.

53 V. Edtmüller, A. Pöthig and T. Bach, *Tetrahedron*, 2017, **73**, 5038–5047.

54 Q. Guo, M. Wang, Q. Peng, Y. Huo, Q. Liu, R. Wang and Z. Xu, *ACS Catal.*, 2019, **9**, 4470–4476.

55 R. Qi, C. Wang, Y. Huo, H. Chai, H. Wang, Z. Ma, L. Liu, R. Wang and Z. Xu, *J. Am. Chem. Soc.*, 2021, **143**, 12777–12783.

56 H. D. Xia, Z. L. Li, Q. S. Gu, X. Y. Dong, J. H. Fang, X. Y. Du, L. L. Wang and X. Y. Liu, *Angew. Chem., Int. Ed.*, 2020, **59**, 16926–16932.

57 Y. Zhang, Y. Sun, B. Chen, M. Xu, C. Li, D. Zhang and G. Zhang, *Org. Lett.*, 2020, **22**, 1490–1494.

58 Y. Li, K. Zhou, Z. Wen, S. Cao, X. Shen, M. Lei and L. Gong, *J. Am. Chem. Soc.*, 2018, **140**, 15850–15858.

59 K. Zhou, Y. Yu, Y.-M. Lin, Y. Li and L. Gong, *Green Chem.*, 2020, **22**, 4597–4603.

60 X. Shen, Y. Li, Z. Wen, S. Cao, X. Hou and L. Gong, *Chem. Sci.*, 2018, **9**, 4562–4568.

61 H. Yu, S. Dong, Q. Yao, L. Chen, D. Zhang, X. Liu and X. Feng, *Chem. – Eur. J.*, 2018, **24**, 19361–19367.

62 K. Zhang, L.-Q. Lu, Y. Jia, Y. Wang, F.-D. Lu, F. Pan and W.-J. Xiao, *Angew. Chem., Int. Ed.*, 2024, **58**, 13375–13379.